The design and fabrication of supramolecular semiconductor nanowires formed by benzothienobenzothiophene (BTBT)-conjugated peptides

Article

Accepted Version

DOI: 10.1002/ ((please add manuscript number))
Article type: Full Paper

Design and Fabrication of Self-Assembled Semiconductor Nanowires Formed by Benzothienobenzothiophene (BTBT)-Conjugated Peptides

Mohammad Aref Khalily, Hakan Usta, Mehmet Özdemir, Gokhan Bakan, Begum Dikecioglu, Aykutlu Dana, Mustafa O. Guler**

Dr. M. A. Khalily, Prof. G. Bakan, B. Dikecioglu, Prof. A. Dana
Institute of Materials Science and Nanotechnology and National Nanotechnology Research Center (UNAM), Bilkent University, Ankara, 06800, Turkey.

Prof. H. Usta, M. Özdemir
Department of Materials Science and Nanotechnology Engineering, Abdullah Gül University, Kayseri, 38080, Turkey.

E-mail: hakan.usta@agu.edu.tr

Prof. G. Bakan

Department of Electrical and Electronics Engineering, Atilim University, Ankara 06836, Turkey.

C. Edwards-Gayle, J. A. Hutchinson, Prof I. W. Hamley
Dept of Chemistry, University of Reading, Whiteknights, Reading RG6 6AD, U.K.

Prof. M.O. Guler
Institute for Molecular Engineering, University of Chicago, Chicago, IL, 60637 USA.

E-mail: mguler@uchicago.edu

Keywords: peptide semiconductor conjugates, synthesis, self-assembly, nanowire, conductivity

The π-conjugated small molecules based on [1]benzothieno[3,2-*b*]benzothiophene (BTBT) unit have attracted immense interest in the field of solution-processable organic semiconductors owing to their record high-performances in organic field-effect transistors (OFETs), and uses in relevant (opto)electronic applications such as photovoltaic devices and flexible displays. Here we report design, synthesis, and self-assembly of two novel β-sheet forming BTBT-peptide conjugates in aqueous media, which assemble into highly uniform semiconductor nanofiber with a diameter of 11-13 (±1) nm and micron-size in length. Spectroscopic characterizations reveal the presence of *J*-type π-π interactions among BTBT molecules within BTBT-peptide nanofibers. Moreover, electrical measurements exhibited remarkable conductivities as high as 6.0×10^{-6} S/cm for BTBT-peptide nanofiber films. BTBT π-core is demonstrated, for the first time, in the formation of self-assembled peptidic nanostructures from aqueous media for potential use in tissue engineering, (opto) electronics, and bioelectronics.

1. Introduction

The π-conjugated small molecules based on [1]benzothieno[3,2-*b*]benzothiophene (BTBT) unit have attracted enormous interest in the field of solution-processable organic semiconductors owing to their record high-performances in organic field-effect transistors (OFETs),[1] and uses in relevant (opto)electronic applications such as photovoltaic devices and flexible displays.[2] Since the first report of BTBT-based semiconductors in 2006 by Takimiya et al.,[3] record high hole mobility of 43 $cm^2/V\cdot s$ (25 $cm^2/V\cdot s$ on average) have been achieved when these *p*-type semiconductors were solution-processed (spin-coated, gravuare-printed, drop-casting, etc.) from organic solvents into thin-films in OFET devices.[4] Compared with most of the previously developed π-conjugated structures, BTBT offers superior structural and electronic properties such as facile synthesis and structural

functionalization, good solubility in organic solvents, high-crystallinity, co-planarity, and impressive charge-transport, which overall make this π-core quite attractive for further applications in (opto)electronic devices; especially, in bioelectronics.

As regard the synthesis/device studies performed on this molecular system, to the best of our knowledge, BTBT π-core has yet to be demonstrated in the formation of electroactive self-assembled one-dimensional (1D) nanowires from aqueous media for potential use in bioelectronics and tissue engineering. Although biomolecular self-assembly has been an attractive tool over the past few decades to fabricate a variety of well-defined supramolecular nanostructures such as micelles, sheets, vesicles, tubes, and fibers,[5] peptide-based supramolecular nanostructures are particularly of great interest due to their biocompatibility, biofunctionality, stimuli responsiveness, and rich functionality.[6] As a result of structural versatility and facile design and synthesis, numerous peptide-based supramolecular nanostructures with various chemical compositions have been developed and extensively studied previously for tissue engineering, drug delivery, sensing, catalysis, optoelectronic and biomedical applications.[6b, 7] Recently, there is also a growing research interest to employ semiconductor-peptide-based self-assembly process in the bottom-up fabrication of supramolecular nanostructured (opto) electronic materials.[6b, 8] In a typical approach, a π-conjugated organic (semi)conductor small molecule is covalently attached to a short self-assembling peptide sequence, and these peptidic organic π-structure amphiphiles self-assemble into well-defined 1D nanostructures under aqueous conditions. This type of electroactive nanostructures formed in aqueous media hold great promise in a variety of applications in (opto) electronics, organic chromophore arrays and bioelectronics.[8-9] Several research groups have previously reported that self-assembling peptide sequences having π-conjugated semiconducting structures can form 1D nanowire. However, only a limited number of π-conjugated systems such as oligothiophenes, naphthalenediimides, pyrenes, and oligo (p-phenylene vinylene) were used in these studies.[8, 10] Therefore, it is still very

important to further investigate new semiconductor structures –especially, the high-performing ones- in the peptidic self-assembly processes to widen the scope of biocompatible (opto)electronic materials. Therefore, we envision that self-assembled nanostructures formed in aqueous media from BTBT-peptide conjugates, which employs charge-transporting BTBT π-units in the hydrophobic core, may pave the way to various applications in bioelectronics. On the other hand, developing a widely applicable synthetic approach to covalently link π-conjugated cores and peptide sequences, without requiring any specific functional group on the semiconductor π-system, would enable further development of novel semiconductor-peptide nanostructures in this field.

Herein, we report design, synthesis, and self-assembly of two novel β-sheet forming semiconductor-peptide amphiphilic molecules **BTBT-Peptide** (BTBT-C_3-COHN-Ahx-VVAGKK-Am) and **C_8-BTBT-Peptide** (C_8-BTBT-C_3-COHN-Ahx-VVAGKK-Am) in aqueous media, which assemble into highly uniform nanofibers with diameter of 11-13(±1) nm and micron-size length as evidenced by atomic force microscope (AFM) and transmission electron microscope (TEM) (**Figure 1**). The self-assembly process and photophysical properties of the corresponding nanofibers are studied, which indicates the formation of J-aggregated BTBT π-cores with extended π-delocalizations in the hydrophobic core. The hydrophobicity of the π-system (BTBT *vs* C_8-BTBT) is found to have a profound effect on the required self-assembly condition. The charge transport characteristics were measured for nanofiber-based peptide films by depositing Au electrodes via thermal evaporation, which yield average electrical conductivities of $4.2(\pm1.8)\times10^{-6}$ S/cm and $2.4(\pm0.47)\times10^{-7}$ S/cm for BTBT-peptide and C8-BTBT-peptide, respectively. The synthesis method employed here to functionalize the BTBT π-core for covalent attachment to the peptide sequence is a two-steps approach, which does not require any pre-existing functional group on the π-system, and it should be broadly applicable to π-conjugated *p*-type organic semiconductors. Herein, BTBT π-core is demonstrated, for the first time, in the form of electroactive self-assembled peptide

nanostructures in aqueous media for potential use in tissue engineering and bioelectronics. The conductive properties were measured as among the highest reported to date for non-doped peptide films.

2. Result and Discussion

2.1. Synthesis of BTBT molecules

The rational design of the new BTBT precursors for peptide attachment is based on the fact that the electronic structure of the [1]benzothieno[3,2-*b*]benzothiophene (BTBT) π-core should not be altered while becoming structurally compatible with solid phase peptide synthesis (SPPS) technique. To this end, we have designed and synthesized two precursors without (2-[1]benzothieno[3,2-b][1]benzothiophenebutyric acid **(BTBT-C_3-COOH**)) and with (7-octyl-2-[1]benzothieno[3,2-b][1]benzothiophenebutyric acid **(C_8-BTBT-C_3-COOH)**) linear alkyl chain (*n*-C_8H_{17}) at BTBT's 7-position (**Scheme 1**). Both derivatives are functionalized with butyric acid (-C_3H_6COOH) at BTBT's 2-position to enable covalent attachment to the peptide. The terminal carboxylic acid groups provide the required functionality to react with the peptide amino (-NH_2) group in the solid phase peptide synthesis (SPPS). In this design, a linear propylene (C_3) spacer was placed between the carboxylic functional group and BTBT π-core to eliminate any inductive or mesomeric effects of electron-withdrawing –COOH group and also to provide structural flexibility (increased degrees of freedom) to BTBT π-core to adapt the optimal stacking conformation in the 1-D nanostructured channel. In the semiconductor-peptide conjugates, **BTBT-Peptide (BTBT-C_3-COHN-Ahx-VVAGKK-Am)** and **C_8-BTBT-Peptide (C_8-BTBT-C_3-COHN-Ahx-VVAGKK-Am)**, both **BTBT-C_3-COOH** and **C_8-BTBT-C_3-COOH** molecules, are covalently attached to a hexapeptide sequence (H_2N-Ahx-VVAGKK-Am) (**Figure 1**). In this molecular design, while VVA moieties promote the formation of β-sheets assisting aggregation, two lysine (KK) amino acids provide positively-charged sites ensuring good

solubility in aqueous media.[11] On the other hand, BTBT π-core serves as both electroactive and hydrophobic segments to derive the hydrophobic collapse of semiconductor-peptide amphiphiles in aqueous media forming 1D nanowires. In addition to the propylene spacer in the BTBT precursor, a six carbon spacer (Ahx) was introduced between BTBT amide group and hexapeptide sequence to allow semiconducting BTBT molecules organize in a favorable supramolecular conformation during self-assembly process.

The synthetic routes to **BTBT-C_3-COOH** and **C8-BTBT-C_3-COOH** are shown in **Scheme 1** and experimental procedures are provided in the experimental section. The synthesis of **BTBT-C_3-COOH** was performed in two steps. BTBT first undergoes a Friedel-Crafts acylation reaction with methyl 4-chloro-4-oxobutyrate in the presence of $AlCl_3$ Lewis catalyst to yield Methyl 2-[1]benzothieno[3,2-b][1]benzothiophenebutyrate (**BTBT-CO-C_2-COOMe**) in 43% yield. Note that this reaction is a selective acylation with the acyl chloride functionality and the methyl ester group in the reagent remains unreacted. Since carbonyl (-CO-) is a well-known electron-withdrawing functionality and can significantly change the electronic structure of BTBT (i.e., π-electron-density, HOMO/LUMO energies, band gap, charge-transport behavior), in the second step, the carbonyl group (-CO-) directly attached to the phenyl ring of the BTBT π-core is converted to methylene (-CH_2-) via Wolf-Kishner reduction reaction in the presence of NH_2NH_2/KOH in diethylene glycol. Note that this reaction condition provides a strongly basic solution to enable simultaneous hydrolysis of the methyl ester to a carboxylate group during the course of this reaction, which upon acidification yields **BTBT-C_3-COOH** in 35% yield. The same two-steps approach was also employed starting with octyl-substituted BTBT **(mono-C_8-BTBT)** in the synthesis of **C_8-BTBT-C_3-COOH**. Note that mono-C_8-BTBT was prepared via Friedel-Crafts acylation of unsubstituted BTBT with octanoyl chloride and a subsequent Wolf-Kishner reduction in 57% total yield. The intermediate compounds and final BTBT-based carboxylic acid containing precursors were purified by silica gel column chromatography, and the chemical structures

and purities were evaluated by $^{1}H/^{13}C$ NMR (**Figure S1 and Figure S2**), mass spectroscopy (ESI) and thin-layer chromatography.

2.2. Synthesis of BTBT-Peptide molecules

The BTBT-Peptide molecules were synthesized by using solid phase peptide synthesis (SPPS) technique. The synthesis were performed on MBHA Rink Amide resin by reacting fluorenylmethyloxycarbonyl (Fmoc) protected amino acids (2.0 equiv.), O-Benzotriazole-N,N,N',N'-tetramethyl-uroniμM-hexafluoro-phosphate (HBTU) (1.95 equiv.) and N,N-diisopropylethylamine (DIEA) (3.0 equiv.) for 6 h in each coupling step. Note that in the final steps of **BTBT-Peptide** and **C_8-BTBT-Peptide** synthesis, 1.5 equivalents of **BTBT-C_3-COOH** and **C8-BTBT-C3-COOH** were added, respectively, and the coupling reactions were performed for additional 24 h. Then, protecting groups were removed and the BTBT-peptides were cleaved from the solid Resin by a mixture of trifluoroacetic acid: triisopropylsilane: water. The BTBT-peptide products precipitated into cold ether. The final products were collected by centrifugation and lyophilization as a white powder. The final BTBT-peptide amphiphiles were purified by preparative high performance liquid chromatography (prep-HPLC) and characterized by liquid chromatography-mass spectrometry (LC-MS) (**Figure S3 and Figure S4**).

2.3. Studying self-assembly of BTBT-Peptide molecules

UV-vis, fluorescence, circular dichroism (CD) and x-ray photoelectron spectroscopies (XPS) were conducted to study self-assembly of BTBT-Peptide at different pH conditions. Absorption of the reference semiconductor C8-BTBT molecule in tetrahydrofuran (THF) and BTBT-Peptide molecule dissolved at pH = 2 showed the same spectra with well-resolved vibronic peaks at 275-350 nm, which can be attributed to π-π^* ($S_0 \rightarrow S_1$) electronic transition of BTBT core (**Figure 2a**). However, upon charge neutralization by increasing the pH value of the solution to 10, a drastic decrease in absorption intensity and a corresponding

broadening were observed along with a ~20 nm red-shift (**Figure 2a**). Meanwhile, the emission profile of BTBT-Peptide at pH = 10 demonstrated broadening and significant red-shift (λ_{em} = 350 nm → 405 nm) in emission signal (**Figure 2b**). The drastic changes in both UV-vis and fluorescence spectra switching from acidic (pH = 2) to basic (pH = 10) media revealed the presence of *J*-type π-π interactions among BTBT molecules.[12] Note that the observed excitonic behavior for the current self-assembled BTBT-peptide molecule is quite different than those of the previously reported vapor-deposited/spin-coated BTBT thin-films, which indicates that somewhat different intermolecular arrangement and packing is achieved within these 1D nanofibers.[2a, 13] Charge repulsions caused by protonated amine groups at acidic media (pH = 2) prevent proper aggregation of BTBT-Peptide molecules, and as a result we observed flat CD signals (**Figure 2c**). When the pH of solution was adjusted to 10, several CD signals appeared. The negative cotton effect in the range of 200-240 nm reveals formation of highly ordered β-sheet secondary structures among BTBT-Peptide molecules (**Figure 2c**).[14] Several other chiral signals were also observed in the range of 240-350 nm, which confirms induction of chirality to achiral BTBT molecules during assembly of BTBT-Peptide molecules at pH = 10. Soluble (pH=2) BTBT-Peptide molecules analyzed by XPS showed the main C 1s peak at ~??? eV corresponding to aliphatic XXX, YYY, and ZZZ bonds. A relatively weaker feature at 292.4 eV was observed, which is found to increase notably along with a slight shift to higher energy (292.6 eV) upon self-assembly at pH=10 (**Figure 2d**). This feature is typically considered to be characteristic of aromatic compounds (π–π* transitions) and indicates the presence of BTBT π-core.[15] Since BTBT is a small molecular π-system, the observed intensity increase and shift could be attributed to (intermolecular) further delocalized π-system in the self-assembled BTBT as a result of molecular stackings in the hydrophobic core.

2.4. Imaging and Scattering of BTBT-Peptide nanofibers

Positively stained self-assembled BTBT-Peptide nanofibers were imaged by transmission electron microscope (TEM) showing formation of well-defined 1D nanofibers having diameters of 11±1 nm and micron-sized lengths (**Figure 3a-b**), which was further confirmed by atomic force microscopy (AFM) images (**Figures 3c-d**). Considering that BTBT-Peptide is functionalized from only one side with a peptide sequence and its modeled molecular length is ~4.4 nm (**Figure S5**) in fully extended conformation, the nanofiber consists of circular alignments of fully extended BTBT-Peptide conjugates perpendicular to the fiber long axis as modeled in **Figure 1b**. SAXS data is shown in Figure S6. A core-shell cylinder model was employed to fit the data, using the software SASfit. For BTBT, the core radius is (2.18 ± 1.00) nm and the shell radius is 0.92 nm, giving a total fibril radius of (3.10 ± 1.00) nm. This is somewhat shorter than the estimated molecular length which suggests that there is some overlapping and/or bending of the hydrophobic BT and alkyl chains in the core of the fibres. For C8-BTBT, the core radius was found to be (2.26 ± 1.00) nm, while the shell thickness is 1.48 nm, giving a total fibre radius of (3.74 ± 1.00) nm. As expected, this is larger than for BTBT. It is interesting that the shell radius is increased, but not the core radius. This suggests that some of the β-sheet peptide sequence forms part of the shell in the fibrils as far as SAXS contrast is concerned. The small core radius indicates again folding or interdigitation of the hydrophobic end groups, even more than for BTBT.

2.5. Studying self-assembly of C_8-BTBT-Peptide molecule

The self-assembly process for C_8-BTBT-Peptide molecule was also studied to observe how enhanced hydrophobicity affects aggregation behavior at different pH conditions. As compared to BTBT-Peptide, C_8-BTBT-Peptide includes a relatively more hydrophobic π-system since it contains a long lipophilic octyl ($-C_8H_{17}$) substituent at BTBT's 7-position. Interestingly, C_8-BTBT-Peptide molecule demonstrated a bathochromic shift ($\Delta\lambda_{onset} \approx 20$ nm) and broadening of absorption bands in both acidic and basic media (**Figure 4a**). Similarly,

the emission maxima exhibited significant red shifts (λ_{em} = 350 nm → 410 nm) of ~60 nm in both acidic and basic conditions (**Figure 4b**). These spectral changes reveal the existence of *J*-type π-π interactions between BTBT molecules at both high and low pH values.[12] Circular dichroism spectroscopy further confirms self-assembly of C_8-BTBT-Peptide molecules in both acidic and basic media showing presence of numerous chiral signals at both pH values of 2 and 10 (**Figure 4c**). While C_8-BTBT-Peptide molecules show β-sheet secondary structure formation at basic condition (pH = 10) along with several other chiral signals, which are attributed to absorption bands of BTBT molecules; at protonated condition (pH = 2) these signals are relatively less pronounced due to presence of charge repulsions among positively charged amine groups (**Figure 3c**). Despite the presence of repulsive Coulombic forces between protonated amine groups at pH = 2, owing to enhanced hydrophobic character of C_8-BTBT-Peptide, hydrophobicity probably dominates Coulombic repulsions to yield aggregation even at acidic media. Again, self-assembled C_8-BTBT-Peptide films prepared at pH=10 exhibited significantly enhanced C 1s π–π* shakeup feature at 292.8 eV, whereas pH=2 sample did not show any peak in this range (**Figure 4d**). This is attributed to the presence of intermolecular delocalized π-system in the self-assembled BTBT as a result of molecular stackings in the hydrophobic core.[15]

2.6. Imaging of C_8-BTBT-Peptide nanofibers

As shown by TEM, uranyl acetate stained C_8-BTBT-Peptide aggregates formed at basic pH values exhibit well-defined 1D nanofibers having diameters of 13±1 nm and micron-sized length (**Figures 5a-b**). As compared to that of the BTBT-Peptide, the diameter increases by ~1-2 nm for C_8-BTBT-Peptide nanofibers agrees well with the computed molecular length increase from BTBT-Peptide (**Figure S5, ~4.4 nm**) to C8-BTBT-Peptide (**Figure S5, ~5.4 nm**), indicating that the substituent(s) on the BTBT π-core directly effects the nanofiber diameter by changing the size of the hydrophobic core. Atomic force microscopy images

further confirmed the presence of well-defined and micron-sized C8-BTBT-Peptide nanofibers (**Figure 5c-d**).

2.7. Electrical measurements of BTBT-Peptide and C_8-BTBT-Peptide films

After studying the self-assembly characteristics of BTBT-Peptide and C8-BTBT-Peptide molecules, we performed electrical measurements for the corresponding nanofiber-based peptide films to assess their charge-transport behaviors. The 30 µL aqueous solutions of BTBT-peptide or C_8-BTBT-peptide samples was drop casted on a piranha-cleaned glass substrate (1.5 cm x 2 cm), which was then exposed to ammonia vapor in a sealed container for 20 min. Then, the samples were dried overnight at 37 ^oC under vacuum. Finally, Au electrodes (50 nm thickness) were deposited through shadow masks by using thermal evaporation technique, which yielded conduction channels of 10-20 µm length and 1-4 mm width (**Figure 6a-b and Figure S6-7**). The current-voltage characteristics of the resulting channels were measured in ambient atmosphere by sweeping voltage between 0-20 V. The resulting current-voltage curves deviate from a linear trend which is expected from an ideal resistor ($I=V/R$, where R is the resistance) (**Figure 6c-d**). The nonlinear I-V curves are attributed to Schottky barrier formation between the electrodes and the films. The Schottky barriers may be present at metal-(*p*-type) semiconductor junctions depending on the relative positions of the metal Fermi level and the organic semiconductor highest occupied molecular orbital (HOMO) energy. For the current semiconductor-peptide systems, since the HOMO energy level of BTBT π-core is stabilized around -5.6 eV,[2a] a certain degree of charge injection barrier could be expected for gold electrodes.[16] The Schottky contacts exhibit rectifying behavior and behave like p-n diodes, thus the current-voltage relation shows an exponential trend: $I = I_o(e^{V/nV_T} - 1)$, where I_o is the reverse bias current, n is the ideality factor, V_T is the thermal voltage (26 mV at room temperature). To extract the film resistance from the measured I-V curves, the Au-film junction is modeled as a diode and the film between the electrodes is modeled as a resistor (**Figure S8**). In this case, the electrical

conduction is limited by the diode owing to its rectifying behavior for small voltage levels, whereas it is limited by the resistor for increasing voltage levels. The resistor-dominated voltage range is found by expressing the applied voltage as the sum of the voltage drops across the diode and the resistor and taking the derivative of the total voltage with respect to current:

$$V = V_D + V_R = nV_T \ln(I/I_o + 1) + IR$$
$$dV/dI = nV_T/I + I_o + R$$

The derivative of total voltage with respect to current shows 1/I trend for low voltage levels and a constant value for increasing voltage levels revealing the resistance between the electrodes (**Figure S9**). Alternatively, inverse of the slope for the linear fit to the I-V points in the resistor-dominated voltage range can be used to extract the resistance value (**Figure 6c**). The effect of Schottky contacts is weaker for C_8-BTBT-peptide film suggesting that the electrical conduction is mostly resistor-dominated (Error! Reference source not found.**d**). The linear regions of the I-V curves are used to calculate the resistances for C_8-BTBT-peptide films film as well.

The resistivity (ρ) and conductivity (σ) for the films are then calculated by accounting for the channel length (L), width (W) and the film thickness (t) following:

$$\frac{1}{\sigma} = \rho = R\frac{t \times W}{L}$$

The film thickness must be measured for each channel, since films exhibit large nonuniformity in thickness across the sample. The nonuniformity of the films is made evident by large variation in the resistance values (**Table S1**). Atomic force microscopy is used for the thickness measurements (**Figure S10**). A step in the film is created by scribing the film for measurements. **Table S1** shows the channel dimensions and measured/calculated electrical properties of 7 devices from each sample. The average conductivity value for BTBT-peptide film is calculated as $4.2(\pm1.8)\times10^{-6}$ S/cm, whereas C_8-BTBT-peptide film is found to be ~20

times more resistive than BTBT-peptide film with an average conductivity of $2.4(\pm0.47)\times10^{-7}$ S/cm. The decrease in conductivity for C_8-BTBT-peptide films as compared with BTBT-peptide films could be attributed to the presence of octyl ($-C_8H_{17}$) chains attached to individual BTBT π-cores, which consists of a large number of insulating C-C and C-H σ-bonds. The presence of π-conjugated BTBT structures without alkyl substituents in the hydrophobic channel of BTBT-peptide film seems to induce more effective charge-transport behavior. Therefore, introducing different alkyl chains to BTBT-peptide molecules could be a facile strategy to fine tune the conductivity of BTBT-peptide nanofibers. Until today, electroactive supramolecular self-assembled 1D nanostructures mainly suffer from low conductivities of 10^{-10}-10^{-9} S/cm in their non-doped states, and conductivities of 10^{-6}-10^{-5} S/cm were obtained only after p- or n-doping with oxidizing or reducing agents.[17] Remarkably, in the present study, we obtained tremendous conductivity as high as 6.0×10^{-6} S/cm without using any doping agent thanks to the rational design of (C_8)BTBT-peptide nanofibers comprised of an excellent *p*-type BTBT semiconductor. It is worth noting that the I-V curves achieved for BTBT-peptide film using Al contacts are similar to what is observed with Au contacts (**Figure S11**). The mean conductivity value for BTBT-peptide film with Al contacts is $2.6(\pm0.9)\times10^{-6}$ S/cm that is within the range obtained for Au electrodes.

Proteins and β-sheet assemblies have shown to be excellent proton conductors.[18] Owning to presence of rich hydrogen bonding, proton accepting and proton donating groups, proteins and β-sheet fibrils may possibly assist effective proton conduction channels by the Grotthuss mechanism.[19] Therefore, we synthesized a control peptide sequence (**Figure S12-S14**) which does not contain electron conducting group to investigate the contribution of proton conduction in BTBT-peptide nanofiber films. The control peptide molecule (KK) was revealed to form β-sheet structures and assemble into well-defined nanofibers at basic media similar to BTBT-peptide conjugates.[11] The KK films were deposited on glass substrates and electrical measurements were conducted under similar conditions as in BTBT-peptide films.

The conductivity results for KK films are summarized in **Table S2** showing an average conductivity value of 1.7×10^{-8} S/cm with $0.6\text{x}10^{-8}$ S/cm standard deviation. BTBT-peptide films demonstrate approximately 200 fold higher conductivity than KK films under same conditions. The enhancement in conductivity can be attributed to electronic conducting nature of BTBT moieties. We can conclude that BTBT-peptide nanofibers exhibit hybrid proton and electron conductivity which is consistent with literature studies.[18b]

3. Conclusion

In summary, we have developed a synthetic approach to modify a benchmark high-performance organic semiconductor, [1]benzothieno[3,2-*b*]benzothiophene (BTBT), to be compatible with SPPS. Two derivatives of BTBT molecules were successfully conjugated to a β-sheet forming peptide having positive charge. The BTBT-peptide molecules are readily soluble in aqueous media forming highly uniform nanofibers with a diameter of 11-13(±1) nm and micron-size length. Spectroscopic characterizations revealed the presence of *J*-type aggregations among BTBT molecules resulting in extended π-delocalization within the hydrophobic part of the BTBT-peptide nanofibers. As a result, electrical measurements exhibited remarkable conductivities as high as 6.0×10^{-6} S/cm for BTBT-peptide films. BTBT π-core is demonstrated, for the first time, in the formation of self-assembled peptide nanostructures from aqueous media for potential use in tissue engineering, (opto)electronics, and bioelectronics with one of the highest conductivity value achieved to date in a non-doped state.

4. Experimental Section

Synthesis of BTBT Precursors (BTBT-C_3-COOH and C_8-BTBT-C_3-COOH) for Covalent Peptide Attachment

Methyl 4-([1]Benzothieno[3,2-b][1]benzothiophen-2-yl)-4-oxobutanoate (BTBT-CO-C_2-COOMe): Into a solution of [1]Benzothieno[3,2-b][1]benzothiophene (1) (250 mg, 1.04 mmol) in dry dichloromethane (25 mL) at -10 °C was added $AlCl_3$ (378.58 mg, 2.84 mmol) under nitrogen, Then, methyl 4-chloro-4-oxobutyrate (187.9 mg, 1.248 mmol) was added dropwise, and the mixture was stirred for 1h at the same temperature. The reaction mixture was allowed to stand without cooling and stirred for 24 h at room temperature. The reaction mixture was next poured into ice-cooled water (150 mL) and the product was extracted with chloroform. The organic phase was washed with water, dried over Na_2SO_4, filtered, and evaporated to dryness. The crude product was then purified by column chromatography on silica gel with chloroform as the eluent, affording methyl 4-([1]Benzothieno[3,2-b][1]benzothiophen-2-yl)-4-oxobutanoate (2) as a white solid (160 mg, 43.4% yield).^{1}H NMR ($CDCl_3$): δ 2.85 (t, 2H, J = 7.0 Hz), 3.45 (t, 2H, J = 7.0 Hz), 3.74 (s, 3H), 7.49 (m, 2H), 7.96 (m, 3H), 8.09 (dd, 1H, J = 1.6 Hz, 8.8 Hz), 8.60 (d, 1H, J = 0.8 Hz) ppm; m.p. 189-190 °C.

4-([1]Benzothieno[3,2-b][1]benzothiophen-2-yl)butanoic acid (BTBT-C_3-COOH): A mixture of methyl 4-([1]Benzothieno[3,2-b][1]benzothiophen-2-yl)-4-oxobutanoate (2) (470 mg, 1.33 mmol), potassium hydroxide (296.68 mg, 5.29 mmol), hydrazine hydrate (50-60%, 1.12 mL, 17.98 mmol) in diethylene glycol (50 mL) was heated to 110 °C for 1 h and then further heated at 210 °C for 5 h. The mixture was then allowed to cool to room temperature and acidified with 4M HCl. Then, water (50 mL) was added and the product was extracted with ethyl acetate. The organic phase was washed with water, dried over Na_2SO_4, filtered, and evaporated to dryness. The crude product was then purified by column chromatography on silica gel with ethyl acetate as the eluent, affording 4-([1]Benzothieno[3,2-b][1]benzothiophen-2-yl)butanoic acid (3) as a white solid (150 mg, 35% yield). ^{1}H NMR (d6-DMSO): δ 1.90 (m, 2H), 2.27 (t, 2H, J = 8.0 Hz), 2.78 (t, 2H, J = 8.0 Hz), 7.37 (d, 1H, J = 8.0 Hz), 7.50 (m, 2H), 7.96 (d, 1H, J = 8.0 Hz), 7.98 (s, 1H), 8.02 (d, 1H, J = 7.0 Hz), 8.14 (d, 1H, J = 8.0 Hz), 12.08 (s, 1H) ppm; ^{13}C NMR (d6-DMSO): δ 26.9, 33.5, 34.9, 121.9, 122.0,

124.2, 124.9, 125.8, 126.7, 130.9, 132.6, 132.9, 133.2, 140.0, 141.9, 142.4, 174.7 ppm; m.p. > 400 °C; MS(ESI) m/z ($[M-H]^+$): calcd. for $C_{18}H_{14}O_2S_2$, 325.04; found, 325.02491.

([1]benzothienopheno[3,2-b]benzothienophene-2-yl)octan-1-one (C_7-CO-BTBT): Into a solution of [1]Benzothieno[3,2-b][1]benzothiophene (1) (2.0 g, 8.32 mmol) in dry dichloromethane 90 mL) at -10 °C was added $AlCl_3$ (1.44 g, 10.82 mmol) under nitrogen, Then, octanoyl chloride (1.73 mL, 9.99 mmol) was added dropwise, and the mixture was stirred for 1h at the same temperature. The reaction mixture was allowed to stand without cooling and stirred for 24h at room temperature. The reaction mixture was next poured into ice-cooled water (150 mL) to give a precipitate. The precipitate was collected by filtration and washed consecutively with water and methanol. The crude product was then purified by column chromatography on silica gel with chloroform as the eluent, affording ([1]benzothienopheno[3,2-b]benzothienophene-2-yl)octan-1-one (4) as a white solid (2.0 g, 65.6% yield). ^{1}H NMR ($CDCl_3$): δ 0.91 (t, 3H, J = 7.0 Hz), 1.29-1.44 (m, 8H), 1.81 (m, 2H), 3.07 (t, 2H, J = 7.2 Hz), 7.48 (m, 2H), 7.94 (m, 3H), 8.05 (dd, 1H, J = 1.5 Hz, 8.0 Hz), 8.55 (s, 1H); m.p. 179-180 °C.

2-octyl[1]benzothieno[3,2-b][1]benzothiophene (C_8-BTBT): A mixture of ([1]benzothienopheno[3,2-b]benzothienophene-2-yl)octan-1-one (4) (1.45 g, 3.96 mmol), potassium hydroxide (611.04 mg, 10.89 mmol), hydrazine hydrate (50-60%, 3.15 mL, 50.49 mmol) in diethylene glycol (50 mL) was heated to 110 °C for 1 h and then further heated at 210 °C for 5 h. The mixture was then allowed to cool to room temperature and filtered to give a crude solid. The crude solid was washed with methanol and dried under vacuum to yield a white solid (1.2 g, 86.3% yield). ^{1}H NMR ($CDCl_3$): δ 0.91 (t, 3H, J = 7.0 Hz), 1.30-1.41 (m, 10H), 1.71 (m, 2H), 2.79 (t, 2H, J = 8.0 Hz), 7.30 (d, 1H, J = 8.0 Hz), 7.41 (d, 1H, J = 8.0 Hz), 7.47 (d, 1H, J = 8.0 Hz), 7.74 (d, 1H, J = 8.0 Hz), 7.80 (d, 1H, J = 8.0 Hz), 7.88 (d, 1H, J = 8.0 Hz), 7.92 (d, 1H, J = 8.0 Hz); m.p. 111-112 °C.

Methyl 4-(2-octyl[1]benzothieno[3,2-b][1]benzothiophen-2-yl)-4-oxobutanoate (C_8-BTBT-CO-C_2-COOMe): Into a solution of 2-octyl[1]benzothieno[3,2-b][1]benzothiophene (5) (1.1 g, 3.12 mmol) in dry dichloromethane (50 mL) at -10 °C was added $AlCl_3$ (1.14 g, 8.52 mmol) under nitrogen, Then, Methyl 4-chloro-4-oxobutyrate (0.56 g, 3.74 mmol) was added dropwise, and the mixture was stirred for 1h at the same temperature. The reaction mixture was allowed to stand without cooling and stirred for 20h at room temperature. The reaction mixture was next poured into ice-cooled water (150 mL) and the product was extracted with chloroform. The organic phase was washed with water, dried over Na_2SO_4, filtered, and evaporated to dryness. The crude product was then purified by column chromatography on silica gel with chloroform as the eluent, affording methyl 4-(2-octyl[1]benzothieno[3,2-b][1]benzothiophen-2-yl)-4-oxobutanoate (6) as a white solid (700 mg, 48% yield).^{1}H NMR ($CDCl_3$): δ 0.90 (t, 3H, J = 7.5 Hz), 1.35 (m, 10H), 1.75 (m, 2H), 2.84 (m, 4H), 3.51 (t, 2H, J = 7.5 Hz), 3.76 (s, 3H), 7.33 (d, 1H, J = 8 Hz), 7.77 (s, 1H), 7.85 (d, 1H, J= 8 Hz), 7.93 (d, 1H, J = 8 Hz), 8.09 (d, 1H, J = 8 Hz), 8.60 (s, 1H) ppm; m.p. 144-145 °C.

4-(2-octyl[1]benzothieno[3,2-b][1]benzothiophen-2-yl)butanoic acid (C_8-BTBT-C_3-COOH): A mixture of methyl 4-(2-octyl[1]benzothieno[3,2-b][1]benzothiophen-2-yl)-4-oxobutanoate (6) (700 mg, 1.50 mmol), potassium hydroxide (335 mg, 5.97 mmol), hydrazine hydrate (50-60%, 1.26 mL, 20.28 mmol) in diethylene glycol (50 mL) was heated to 110 °C for 1 h and then further heated at 210 °C for 5 h. The mixture was then allowed to cool to room temperature and acidified with 4 M HCl. Then, water (50 mL) was added and the product was extracted with chloroform. The organic phase was washed with water, dried over Na_2SO_4, filtered, and evaporated to dryness. The crude product was then purified by column chromatography on silica gel with ethyl acetate as the eluent, affording 4-(2-octyl[1]benzothieno[3,2-b][1]benzothiophen-2-yl)butanoic acid (7) as an off-white solid (140 mg, 21.3% yield). ^{1}H NMR (d6-DMSO): δ 0.86 (t, 3H, J = 7.0 Hz), 1.31 (m, 10H), 1.65 (m,

2H), 1.90 (m, 2H), 2.70 (t, 2H, J = 7.5 Hz), 2.75 (m, 4H), 7.35 (m, 2H), 7.94 (m, 4H) ppm. m.p. 186-187 °C; MS(ESI) m/z ($[M-H]^+$): calcd. for $C_{26}H_{30}O_2S_2$, 437.17; found, 437.25624.

Synthesis of BTBT-Peptide Molecules: All peptide molecules were synthesized by using solid phase peptide synthesis (SSPPS) method. The synthesis were performed on MBHA Rink Amide resin and 2 equivalents of fluorenylmethyloxycarbonyl (Fmoc) protected amino acids, 1.95 equivalents of O-Benzotriazole-N,N,N',N'-tetramethyl-uroniμM-hexafluoro-phosphate (HBTU) and 3 equivalents of N,N-diisopropylethylamine (DIEA) for 6 h. Fmoc protecting groups were removed by 20% of piperidine in dimethylformamide for 20 min. The peptides were cleaved from the solid Resin by a mixture of trifluoroacetic acid: triisopropylsilane: H_2O in the ratio of 95:2.5:2.5 for 2 h. The product was collected into a round bottom flask by washing the resin with DCM. The DCM was evaporated by rotary evaporation and cold ether was poured to precipitate the peptide. The final product was collected by centrifuging and then lyophilizing for 72 h to get a white powder.

Synthesis of BTBT-Peptide molecule: In the last step of the synthesis, 1.5 equivalents of BTBT-C_3-COOH were used and the coupling was left for 24 h.

Synthesis of C8-BTBT-Peptide molecule: In the last step of the synthesis, 1.5 equivalents of C_8-BTBT-C_3-COOH were used and the coupling was left for 24 h.

Preparative High Performance Liquid Chromatography: In purification of positively charged peptide molecules, reverse phase silica column (C18) and 0.1% TFA in water and 0.1% in ACN were used as eluents. Preparative liquid chromatography system (Prep-HPLC Agilent 1200 series) integrated with a sample collector was used.

Liquid Chromatography-Mass Spectrometry (LC-MS): After purification of the peptide molecules by Prep HPLC, the mass and purity of the molecules was determined by Agilent Technologies 6530 Accurate-Mass Q-TOF LC-MS. Zorbax SB-C18 column and 0.1% formic acid in water and 0.1% formic acid in acetonitrile were used as mobile phase for positively charged molecules. All peptides were obtained with high purity.

UV-Vis Spectroscopy: The peptide solutions were prepared in a 3 mL quartz cell having 1 cm path length. Stock solutions of BTBT-peptide and C_8-BTBT-peptide were prepared in dd water. 3 mL of BTBT-peptide and C_8-BTBT-peptide having a concentration of 860 μM was prepared from stock solution. The pH of solutions was adjusted to 2 by addition of 1M HCl and to 10 by addition of 1M NaOH. The absorbance values were recorded on CaryBio100 instrument.

Fluorescence Spectroscopy: The peptide solutions were prepared in a 3 mL quartz cell having 1 cm path length. Stock solution of BTBT-peptide and C_8-BTBT-peptide was prepared in dd water. 3 mL of BTBT-peptide and C_8-BTBT-peptide having a concentration of 860 μM was prepared from stock solution. The pH of solutions was adjusted to 2 by addition of 1 M HCl and to 10 by addition of 1 M NaOH. The samples were excited at 310 nm with excitation slit and emission slit widths of 5 and 5 respectively. The emission intensities were recorded on Fluorescence Spectrometer (Cary Eclipse) instrument.

Circular Dichroism (CD) Spectroscopy: The peptide solutions were prepared in a 3 mL quartz cell having 1 cm path length. Stock solution of BTBT-peptide and C_8-BTBT-peptide was prepared in dd water. 3 mL of BTBT-peptide and C_8-BTBT-peptide having a concentration of 860 μM was prepared from stock solution. The pH of solutions was adjusted to 2 by addition of 1 M HCl and to 10 by addition of 1 M NaOH. The samples were measured from 500 nm to 190 nm with 0.1 data pitch, 100 nm/min scanning speed, 1 nm band width and 4 s D.I.T. Average of two measurements were adjusted and sensitivity was selected as standard. All measurements were recorded on Jasco J-815 circular dichroism spectrometer.

X-ray Photoelectron Spectroscopy (XPS): 30 μL of BTBT-peptide and C_8-BTBT-peptide solutions (1 wt %) were dropped on piranha cleaned glass slides (1.5x2 cm^2) and then placed in a sealed container containing 2 mL of NH_4OH solution. After 20 minutes of exposure to NH_3 vapor, the samples were dried at 37 ^oC under vacuum overnight. BTBT-peptide and C_8-BTBT-peptide solutions were prepared at pH 2 then drop casted on glass slides and then dried

at 37 ^{o}C under vacuum overnight. Both assembled and unassembled peptide films were analyzed by Thermo K-alpha monochromatic high-performance X-ray photoelectron spectrometer.

Transmission Electron Microscopy (TEM): 10 μL of BTBT-peptide and C_8-BTBT-peptide solutions were dropped on a carbon grid followed by staining the samples by 2% uranyl acetate solution. Air dried samples were imaged by FEI Tecnai G2 F30 transmission electron microscope.

Atomic Force Microscopy (AFM): Peptide samples were prepared on silicon wafer using 5 μL of 200 fold diluted from stock solutions (1 % w/v). The pH of peptide solutions was adjusted to 10 by addition of 1M NaOH. After dropping the solution onto a silicon wafer, the samples were air-dried. Tapping mode imaging were used to image topography of the resulting samples, using appropriate cantilevers (force constant of 5 N/m, resonance frequency of f_0=150 kHz). Images were taken in 5 μm or 2 μm areas at a scan rate of 1.5 Hz and a resolution of 512 x 512 points and lines, respectively.

Small-Angle X-ray Scattering Measurements: Experiments were performed on beamline BM29 at the European Synchrotron Radiation Source (ESRF, Grenoble, France). Samples were loaded into PCR tubes in an sample changer rack in an EMBL BioSAXS robot system and were delivered via syringe into a capillary for repeated exposure (with sample translation for each exposure). The X-ray wavelength was 0.0992 nm and the sample-detector distance was 2.867 m. The data were collected on a Pilatus 1M detector and processed and reduced using the beamline software and SAXSUtilities.

Conductivity Measurements: 30 μL of BTBT-peptide, C_8-BTBT-peptide and KK solutions (1 wt%) were dropped on piranha cleaned glass substrates with 1.5 x 2 cm^2 dimensions and then placed in a sealed container containing 2 mL of NH_4OH solution. After 20 min of exposure to NH_3 vapor, the samples were dried at 37 ^{o}C under vacuum overnight. Deposited peptide films were used for electrical characterization. 20 pairs of Au electrodes are formed on each film by

thermal evaporation of Au through shadow masks. The channels have 10 or 20 μm length and 1 mm or 4 mm width (Figure S6 and S7). Gold is chosen as the electrode material as it is commonly used with similar organic films. The shadow masks are obtained from Ossila Ltd. Au is evaporated on the films at a rate of 0.2 nm/s in a thermal evaporation chamber under 3.5×10^{-6} Torr pressure. The final electrode thickness is 50 nm. The electrodes without a channel show resistance levels of a few Ω that is orders of magnitude smaller than the film resistance between the electrodes which is expected to be more than MΩ. For electrical measurements, two tungsten needles attached to separated micro-manipulators are used to touch the Au electrodes with dimensions of 1x1 mm^2 under a probe station. Current through the channel is measured by monitoring the current leaving/entering the probes while sweeping the voltage difference across the electrodes from 0 to 20 V (Figure S8). Current- voltage (I-V) characteristics are then plotted for resistance analysis.

Supporting Information
Supporting Information is available from the Wiley Online Library or from the author.

Acknowledgements

TUBITAK etc. ((Acknowledgements, general annotations, funding. Other references to the title/authors can also appear here, such as "Author 1 and Author 2 contributed equally to this work.")) The work of IWH was supported by EPSRC Platform Grant EP/L020599/1. We thank the ESRF for the award of beamtime (ref. MX-1918).

Received: ((will be filled in by the editorial staff))
Revised: ((will be filled in by the editorial staff))

Published online: ((will be filled in by the editorial staff))

References

[1] aS. Fabiano, H. Usta, R. Forchheimer, X. Crispin, A. Facchetti, M. Berggren, *Adv Mater* **2014**, *26*, 7438-7443; bM. Ozdemir, D. Choi, G. Kwon, Y. Zorlu, B. Cosut, H. Kim, A. Facchetti, C. Kim, H. Usta, *Acs Appl Mater Inter* **2016**, *8*, 14077-14087.

[2] aH. Ebata, T. Izawa, E. Miyazaki, K. Takimiya, M. Ikeda, H. Kuwabara, T. Yui, *J Am Chem Soc* **2007**, *129*, 15732-+; bV. Figa, C. Chiappara, F. Ferrante, M. P. Casaletto, F. Principato, S. Cataldo, Z. Chen, H. Usta, A. Facchetti, B. Pignataro, *J Mater Chem C* **2015**, *3*, 5985-5994; cR. Ozdemir, D. Choi, M. Ozdemir, G. Kwon, H. Kim, U. Sen, C. Kim, H. Usta, *J Mater Chem C* **2017**, *5*, 2368-2379; dK. Takimiya, S. Shinamura, I. Osaka, E. Miyazaki, *Adv Mater* **2011**, *23*, 4347-4370.

[3] K. Takimiya, H. Ebata, K. Sakamoto, T. Izawa, T. Otsubo, Y. Kunugi, *J Am Chem Soc* **2006**, *128*, 12604-12605.

[4] Y. Yuan, G. Giri, A. L. Ayzner, A. P. Zoombelt, S. C. Mannsfeld, J. Chen, D. Nordlund, M. F. Toney, J. Huang, Z. Bao, *Nature communications* **2014**, *5*, 3005.

[5] aH. Gradiar, R. Jerala, *J Nanobiotechnol* **2014**, *12*; bP. W. K. Rothemund, *Nature* **2006**, *440*, 297-302; cG. C. L. Wong, J. X. Tang, A. Lin, Y. L. Li, P. A. Janmey, C. R. Safinya, *Science* **2000**, *288*, 2035-+; dL. H. Yang, H. J. Liang, T. E. Angelini, J. Butler, R. Coridan, J. X. Tang, G. C. L. Wong, *Nat Mater* **2004**, *3*, 615-619.

[6] aE. Arslan, I. C. Garip, G. Gulseren, A. B. Tekinay, M. O. Guler, *Advanced healthcare materials* **2014**, *3*, 1357-1376; bM. S. Ekiz, G. Cinar, M. A. Khalily, M. O. Guler, *Nanotechnology* **2016**, *27*.

[7] aH. Hosseinkhani, P. D. Hong, D. S. Yu, *Chem Rev* **2013**, *113*, 4837-4861; bG. Wei, Z. Su, N. P. Reynolds, P. Arosio, I. W. Hamley, E. Gazit, R. Mezzenga, *Chemical Society reviews* **2017**, *46*, 4661-4708.

[8] J. D. Tovar, *Accounts Chem Res* **2013**, *46*, 1527-1537.

[9] H. A. M. Ardona, J. D. Tovar, *Bioconjugate Chem* **2015**, *26*, 2290-2302.

[10] aG. L. Eakins, R. Pandey, J. P. Wojciechowski, H. Y. Zheng, J. E. A. Webb, C. Valery, P. Thordarson, N. O. V. Plank, J. A. Gerrard, J. M. Hodgkiss, *Adv Funct Mater* **2015**, *25*, 5640-5649; bM. A. Khalily, G. Bakan, B. Kucukoz, A. E. Topal, A. Karatay, H. G. Yaglioglu, A. Dana, M. O. Guler, *ACS nano* **2017**, *11*, 6881-6892.

[11] M. A. Khalily, M. Goktas, M. O. Guler, *Org Biomol Chem* **2015**, *13*, 1983-1987.

[12] H. Shao, T. Nguyen, N. C. Romano, D. A. Modarelli, J. R. Parquette, *J Am Chem Soc* **2009**, *131*, 16374-+.

[13] M. Yilmaz, M. Ozdemir, H. Erdogan, U. Tamer, U. Sen, A. Facchetti, H. Usta, G. Demirel, *Adv Funct Mater* **2015**, *25*, 5669-5676.

[14] M. A. Khalily, G. Gulseren, A. B. Tekinay, M. O. Guler, *Bioconjugate Chem* **2015**, *26*, 2371-2375.

[15] aY. X. Liu, Z. J. Du, Y. Li, C. Zhang, C. J. Li, X. P. Yang, H. Q. Li, *J Polym Sci Pol Chem* **2006**, *44*, 6880-6887; bF. Khelifa, S. Ershov, Y. Habibi, R. Snyders, P. Dubois, *Acs Appl Mater Inter* **2013**, *5*, 11569-11577.

[16] E. H. Rhoderick, *Iee Proc-I* **1982**, *129*, 1-14.

[17] aY. K. Che, A. Datar, K. Balakrishnan, L. Zang, *J Am Chem Soc* **2007**, *129*, 7234-+; bT. Kitamura, S. Nakaso, N. Mizoshita, Y. Tochigi, T. Shimomura, M. Moriyama, K. Ito, T. Kato, *J Am Chem Soc* **2005**, *127*, 14769-14775; cS. K. M. Nalluri, N. Shivarova, A. L. Kanibolotsky, M. Zelzer, S. Gupta, P. W. J. M. Frederix, P. J. Skabara, H. Gleskova, R. V. Ulijn, *Langmuir* **2014**, *30*, 12429-12437; dX. Sun, G. Q. Lai, Z. F. Li, Y. W. Ma, X. Yuan, Y. J. Shen, C. Y. Wang, *Beilstein J Org Chem* **2015**, *11*, 2343-2349.

[18] aN. Amdursky, X. H. Wang, P. Meredith, D. D. C. Bradley, M. M. Stevens, *Adv Mater* **2016**, *28*, 2692-2698; bM. Amit, S. Appel, R. Cohen, G. Cheng, I. W. Hamley, N. Ashkenasy, *Adv Funct Mater* **2014**, *24*, 5873-5880; cD. D. Ordinario, L. Phan, W. G. Walkup, J. M. Jocson, E. Karshalev, N. Husken, A. A. Gorodetsky, *Nat Chem* **2014**, *6*, 597-603; dO. Silberbush, M. Amit, S. Roy, N. Ashkenasy, *Adv Funct Mater* **2017**, *27*.

[19] S. Cukierman, *Biochimica et biophysica acta* **2006**, *1757*, 876-885.

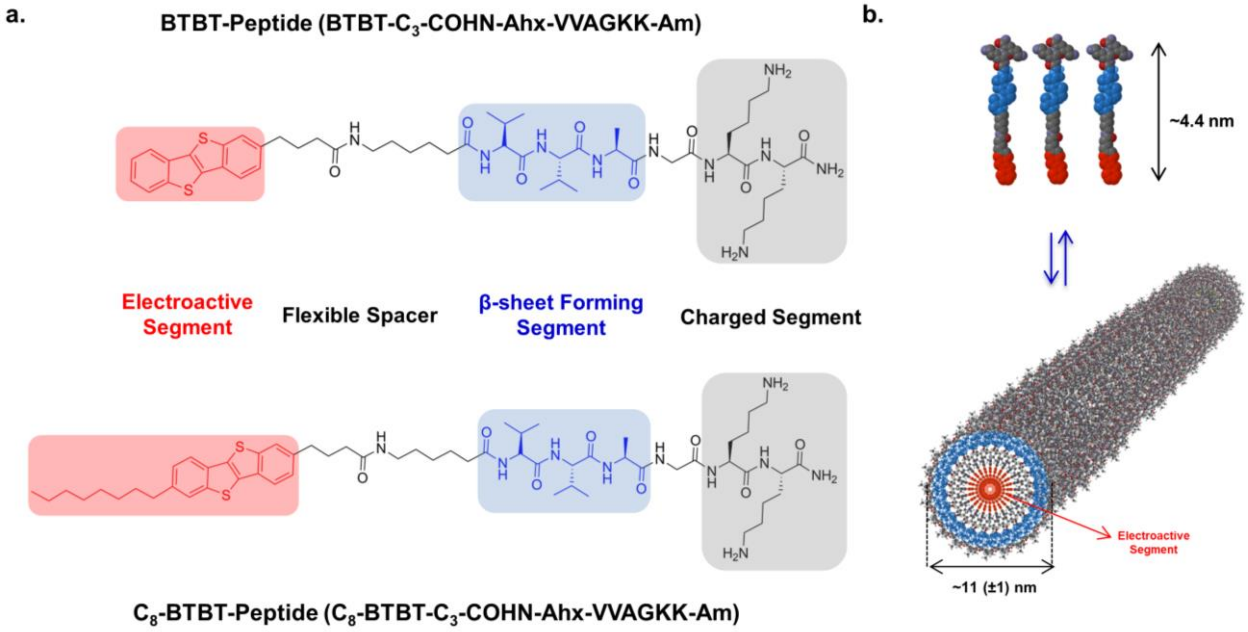

Figure 1. (a) Molecular structures of the [1]benzothieno [3, 2-*b*] benzothiophene (BTBT)-peptide amphiphiles **BTBT-Peptide** (BTBT-C_3-COHN-Ahx-VVAGKK-Am) and **C_8-BTBT-Peptide** (C_8-BTBT-C_3-COHN-Ahx-VVAGKK-Am). (b) Schematic presentation of the self-assembly process for **BTBT-Peptide** amphiphile showing the proposed nanofiber structure with the computed molecular length (~4.4 nm) and the measured nanofiber diameter (~11±1 nm).

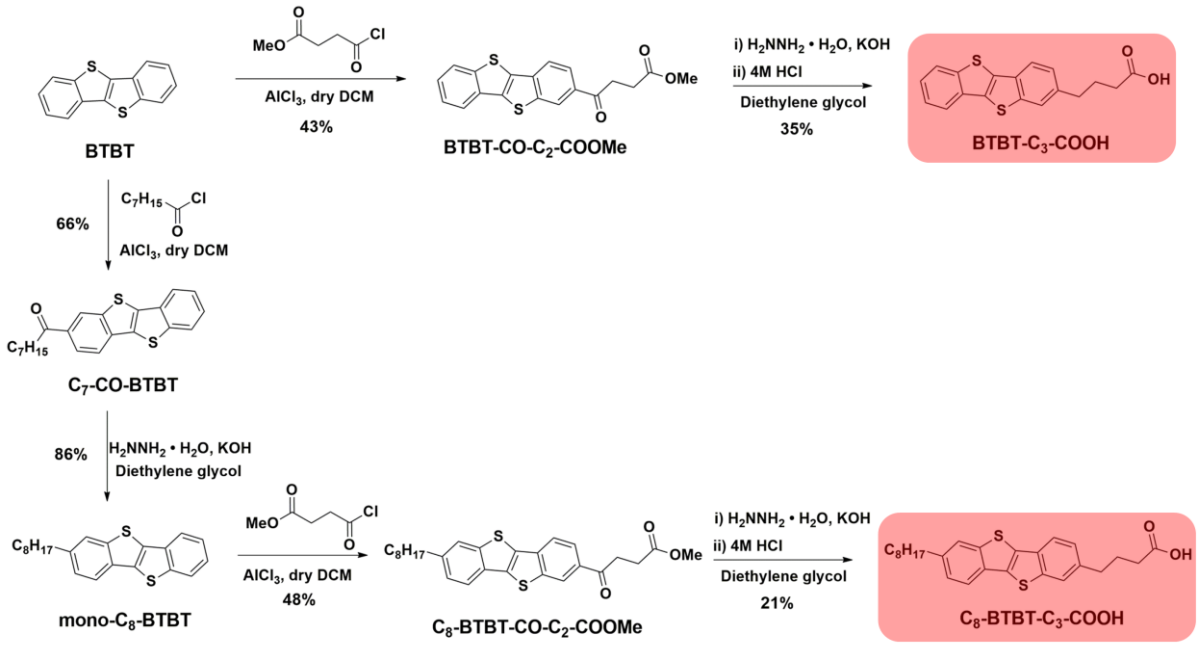

Scheme 1. Synthetic routes to **BTBT-C_3-COOH** and **C_8-BTBT-C_3-COOH**.

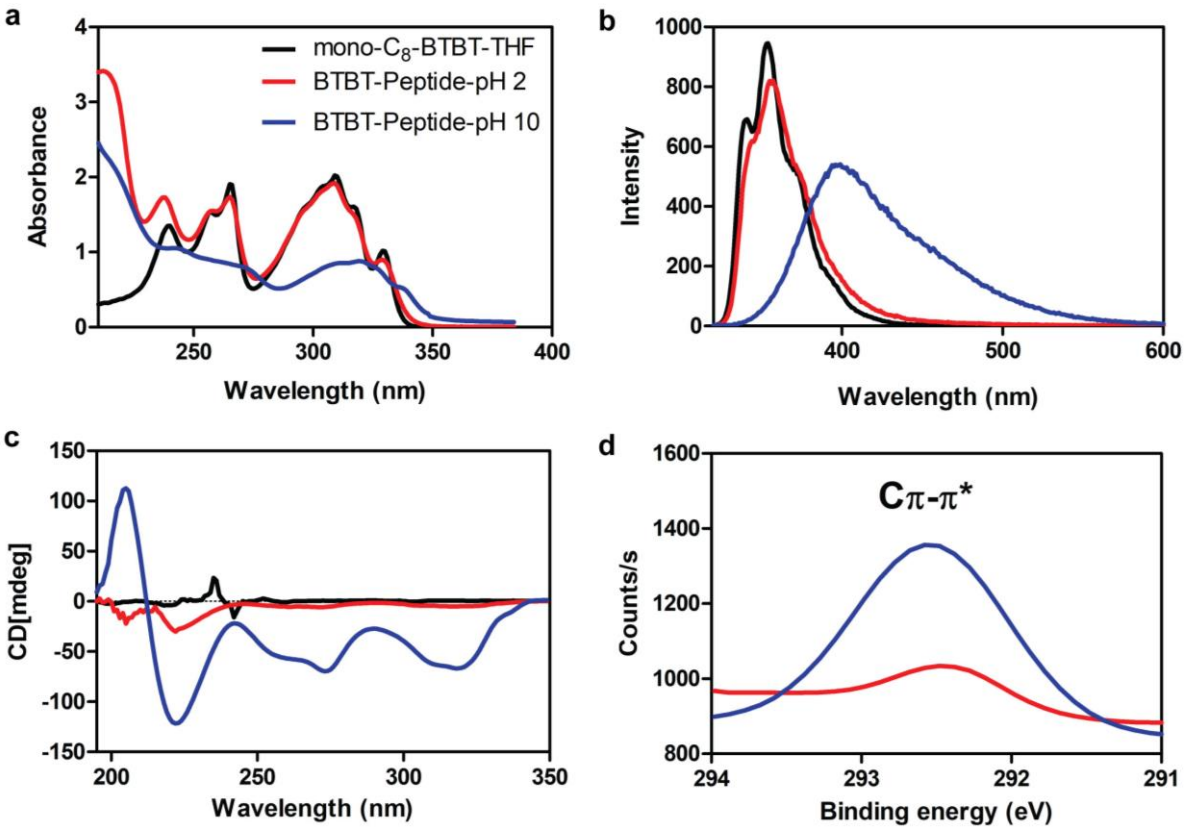

Figure 2. Spectroscopic characterization of BTBT-Peptide self-assembly at different pH conditions. (a) UV-vis absorption (b) fluorescence emission spectra (λ_{ex} = 310 nm) and (c) CD spectrum. (d) XPS spectrum of C1s for BTBT-Peptide films prepared at pH=2 and pH=10.

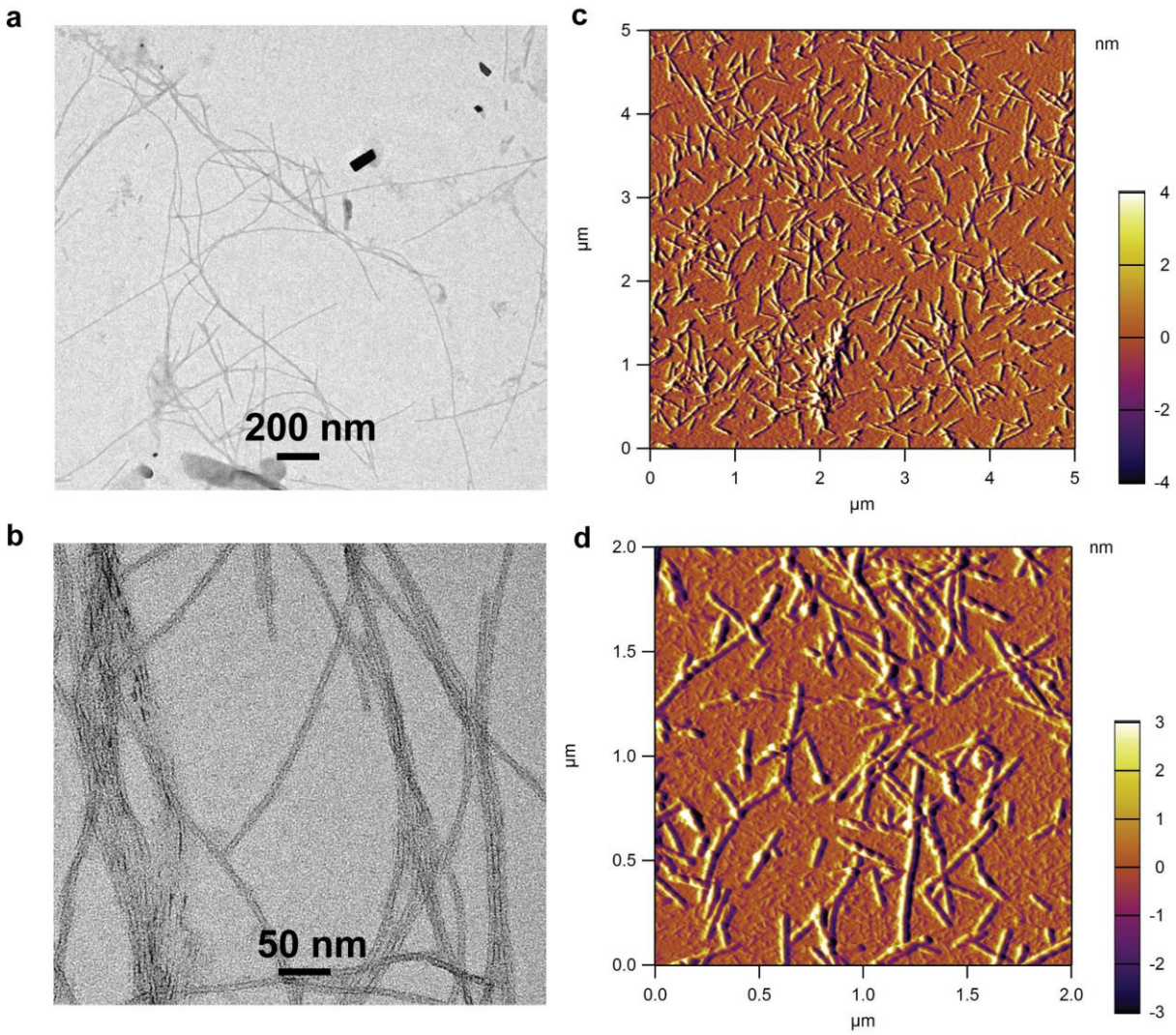

Figure 3. Imaging of BTBT-Peptide molecule. TEM (a and b) and AFM images (c and d) of BTBT-Peptide nanofibers.

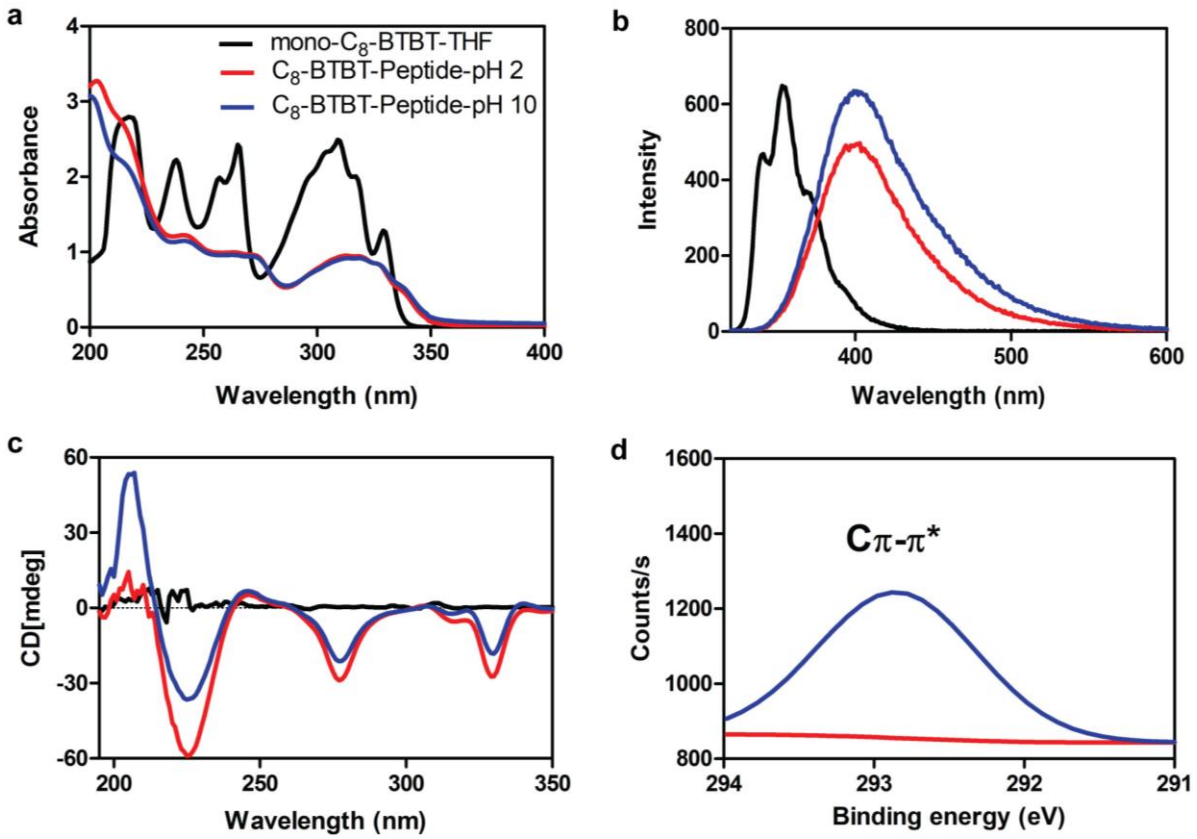

Figure 4. Spectroscopic characterization of C_8-BTBT-Peptide self-assembly at different pH conditions. (a) UV-vis absorption (b) fluorescence emission spectra (λ_{ex}= 310 nm) and (c) CD spectrum. (d) XPS spectrum of C1s for C_8-BTBT-Peptide films prepared at pH=2 and pH=10.

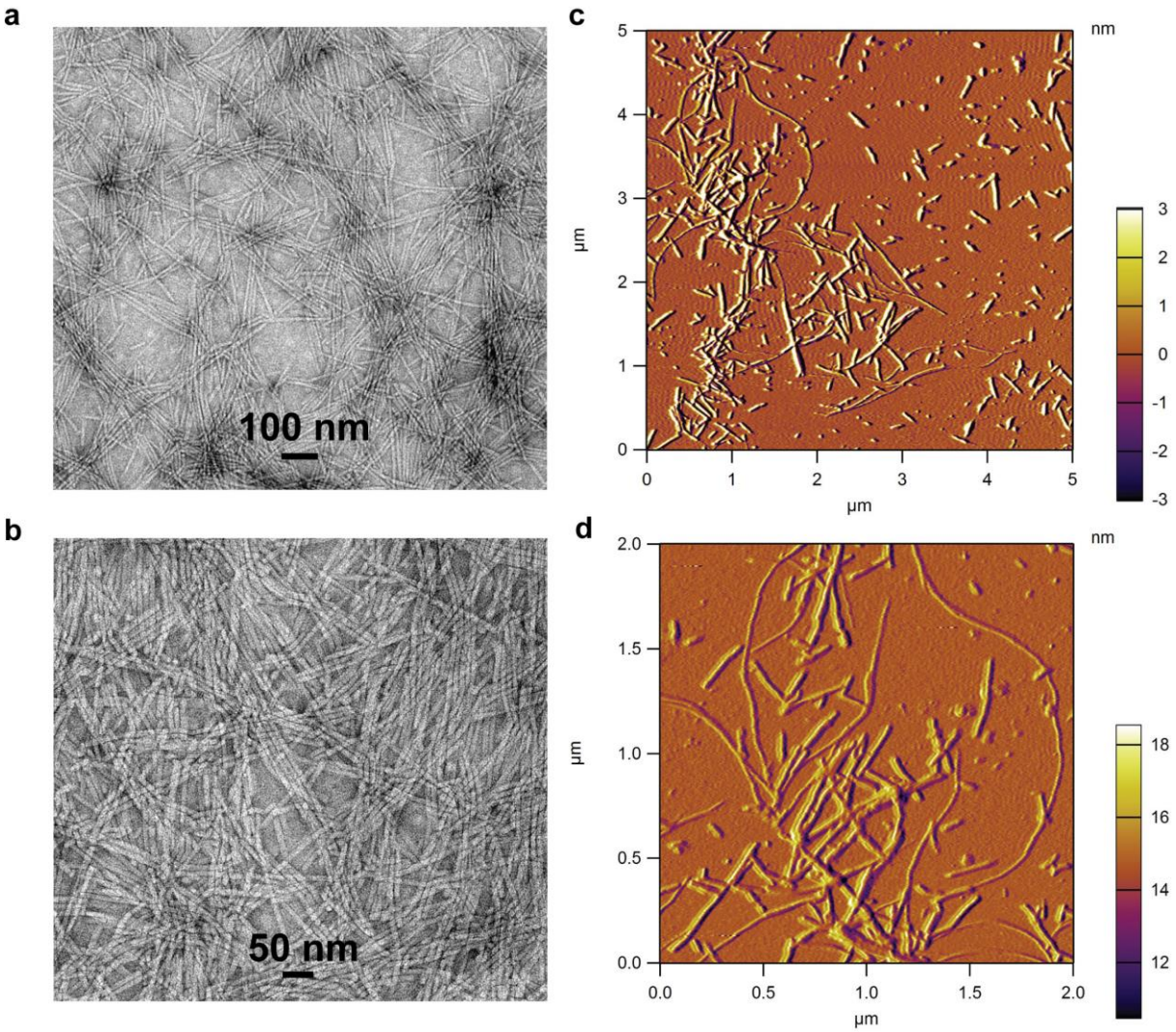

Figure 5. Imaging of C_8-BTBT-peptide molecule. TEM (a and b) and AFM (c and d) images of C_8-BTBT-Peptide nanofibers.

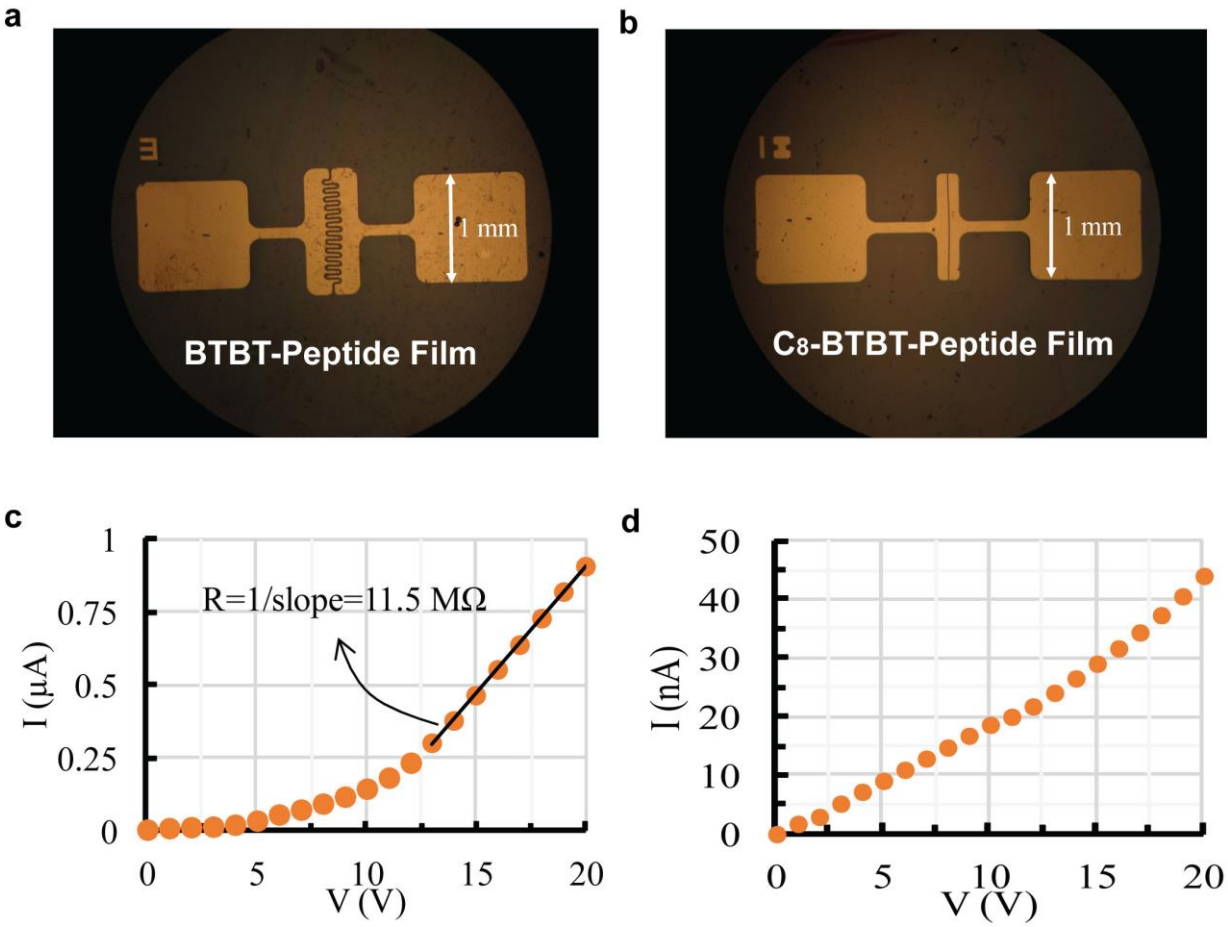

Figure 6. Optical microscope images of Au contacts on BTBT-peptide film with L = 20 μm and W= 4 mm (a) and C_8-BTBT-peptide film with L = 10 μm and W= 1 mm (b). I-V characteristics of BTBT-peptide (c) and C_8-BTBT-peptide films between two Au electrodes (d).

Fabrication of biocompatible supramolecular 1D semiconductor nanowires is demonstrated. Benzothienobenzothiophene (BTBT) – peptide conjugates are synthesized and studied their self-assembly in aqueous media. BTBT– peptide conjugates self-assemble into highly uniform nanowires with diameters of 11-13(±1) nm and micron-sized lengths in aqueous media. BTBT-peptide films exhibit remarkable conductivities as high as 6.0×10^{-6} S/cm.

Peptide semiconductor conjugates, synthesis, self-assembly, nanowire, conductivity

M. A. Khalily, H. Usta*, M. Özdemir, G. Bakan, B. Dikecioglu, A. Dana, M. O. Guler*

Design and Fabrication of Self-Assembled Semiconductor Nanowires Formed by Benzothienobenzothiophene (BTBT)-Conjugated Peptides

ToC figure ((Please choose one size: 55 mm broad × 50 mm high **or** 110 mm broad × 20 mm high. Please do not use any other dimensions))

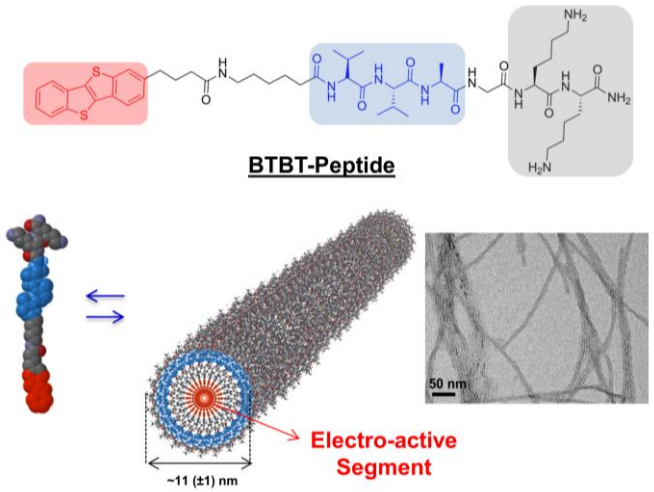

Supporting Information

Design and Fabrication of Self-Assembled Semiconductor Nanowires Formed by Benzothienobenzothiophene (BTBT)-Conjugated Peptides

Mohammad Aref Khalily, Hakan Usta, Mehmet Özdemir, Gokhan Bakan, Begum Dikecioglu, Aykutlu Dana, Mustafa O. Guler**

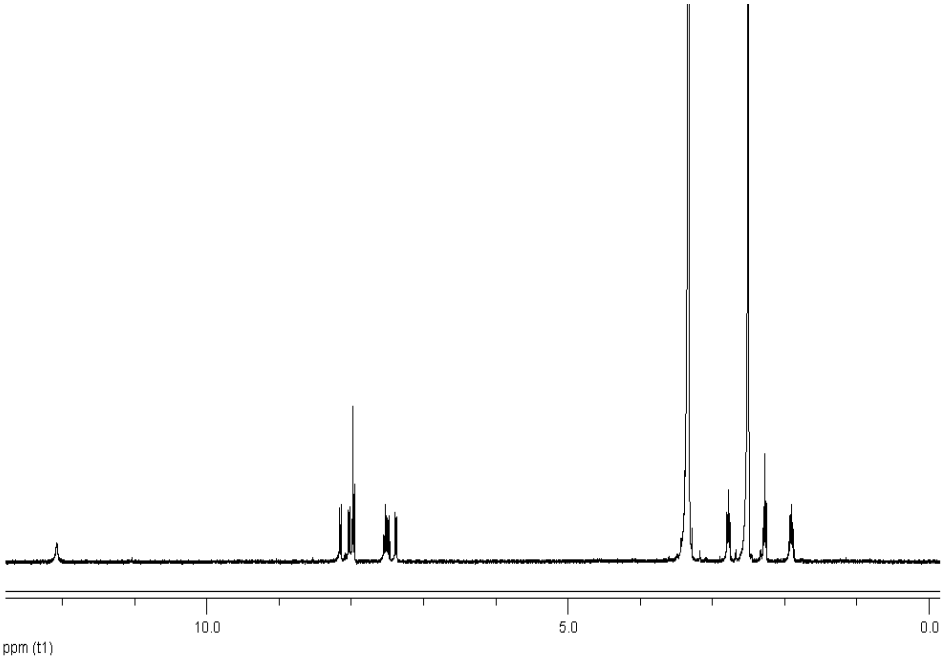

Figure S1. ^{1}H NMR spectra of BTBT-C_3-COOH in dimethyl sulfoxide-d_6.

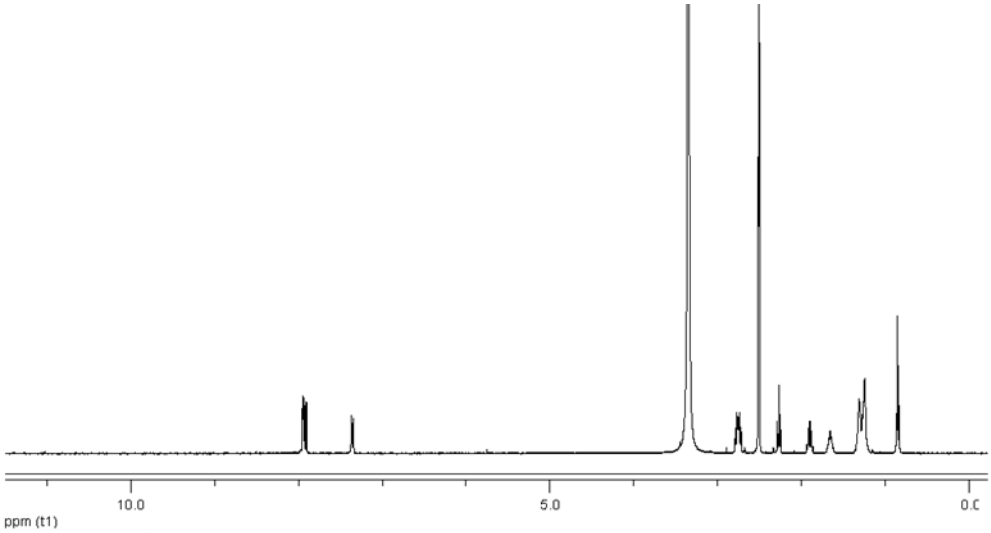

Figure S2. ^{1}H NMR spectra of C_8-BTBT-C_3-COOH in dimethyl sulfoxide-d_6.

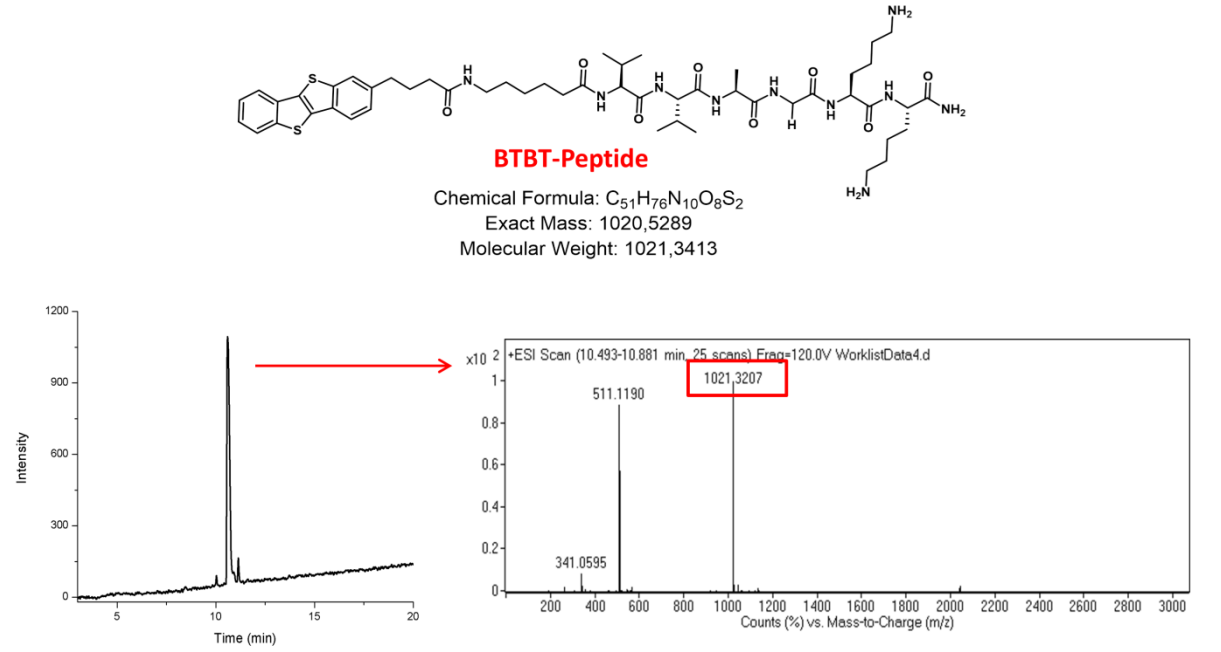

Figure S3. Chemical structure of BTBT-Peptide molecule (top). Liquid chromatogram (left) and mass spectrum (right) of BTBT-Peptide molecule.

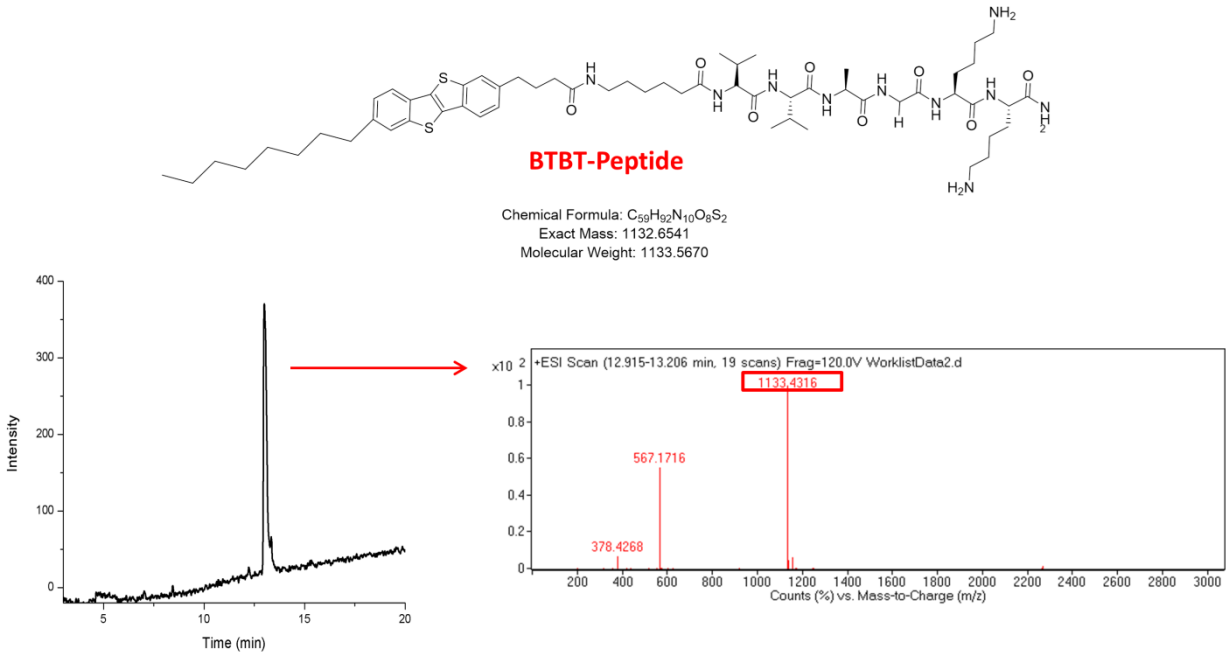

Figure S4. Chemical structure of C_8-BTBT-Peptide molecule (top). Liquid chromatogram (left) and mass spectrum (right) of C_8-BTBT-Peptide molecule.

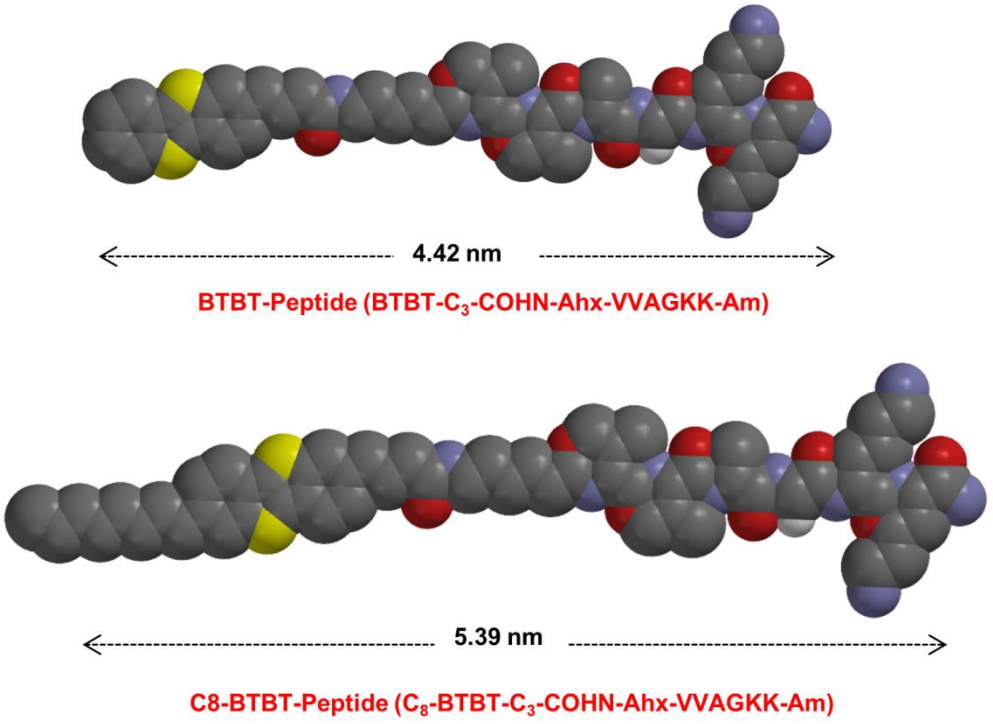

Figure S5. Computed (DFT, B3LYP/6-31G**) molecular lengths of BTBT-Peptide and C8-BTBT-Peptide in their fully extended molecular conformations.

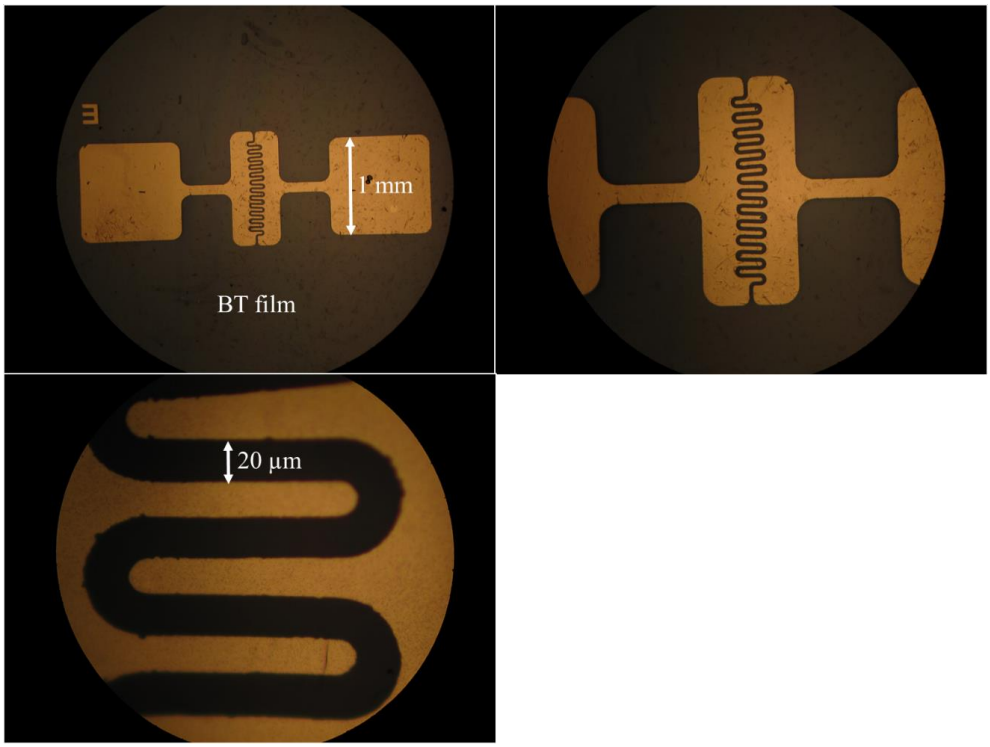

Figure S6. Optical microscope images of Au contacts on BTBT-peptide film with L = 20 µm and W= 4 mm.

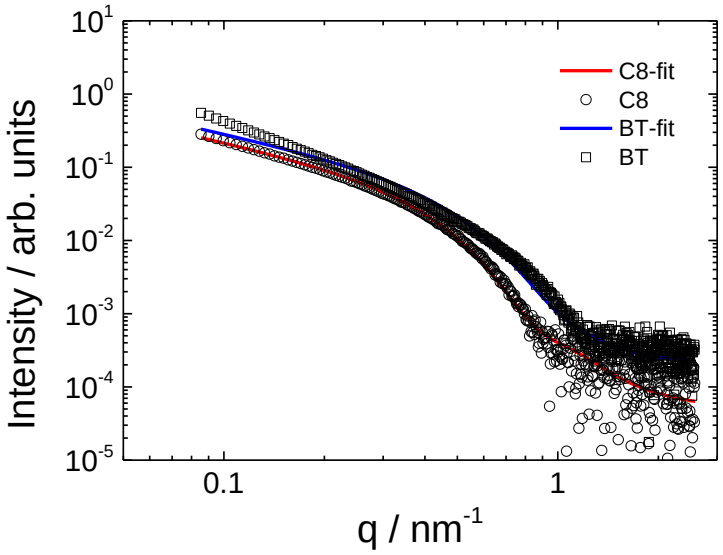

Fig.S6 SAXS data measured for solutions of BTBT and C8-BTBT (open sumbols) along with form factor fits (lines) using a core-shell cylinder model (described in the text)

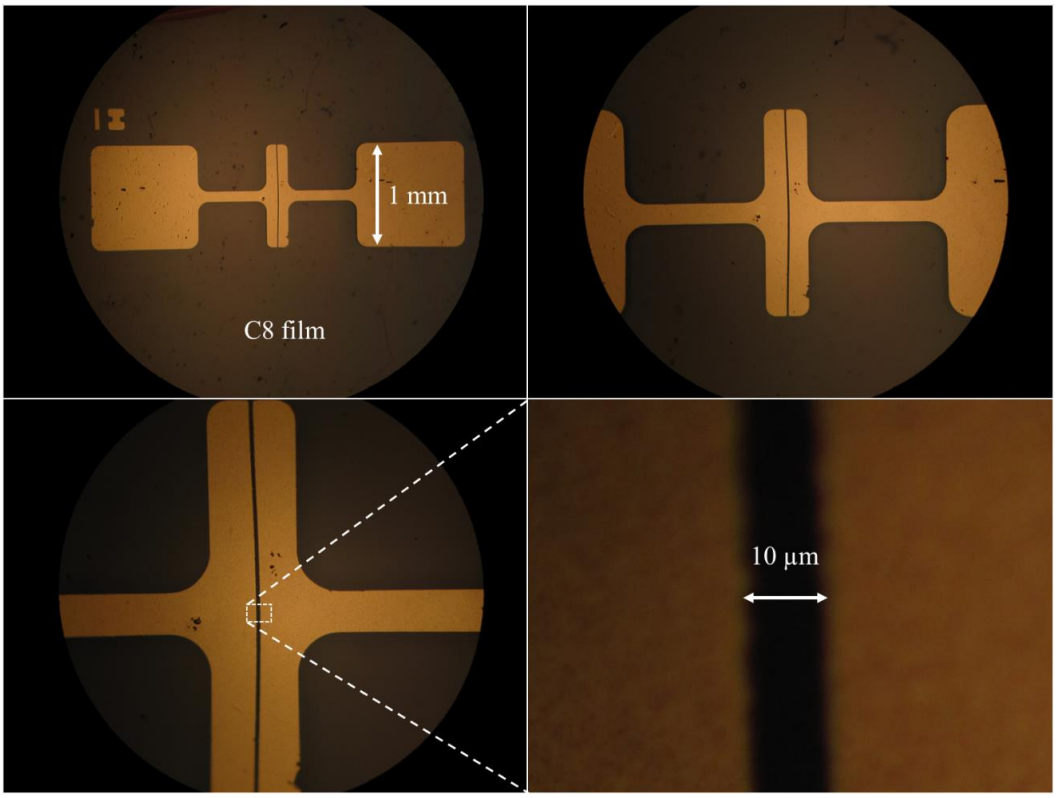

Figure S7. Optical microscope images of Au contacts on C_8-BTBT-peptide film with L = 10 µm and W= 1 mm.

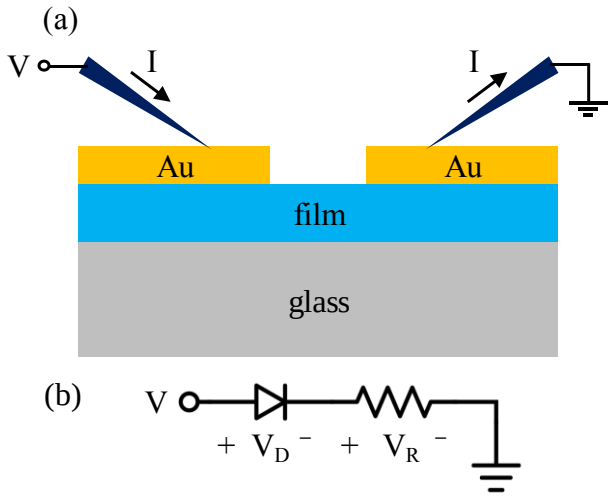

Figure S8. (a) Electric bias/current configurations on cross section illustration of a channel separating Au electrodes. (b) Electrical circuit model of the channel.

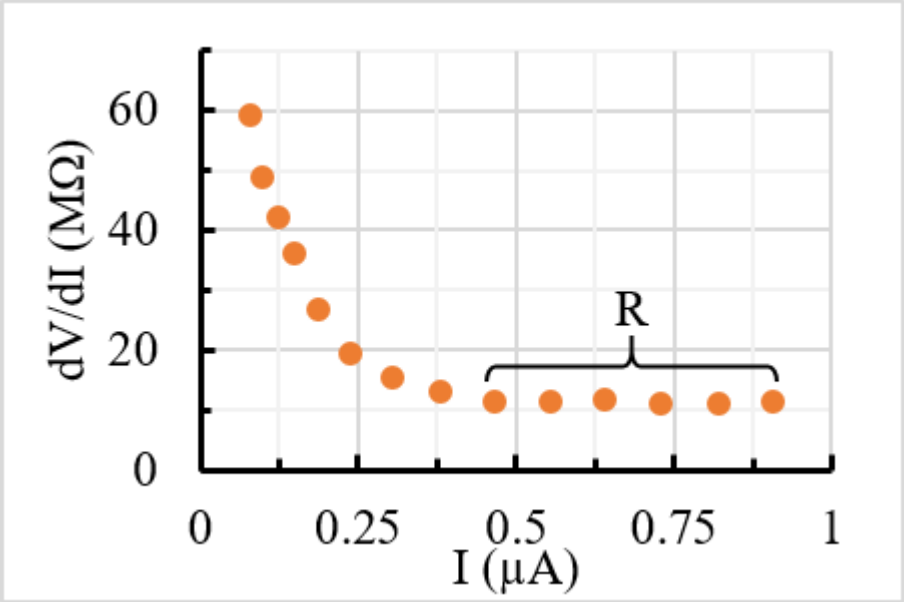

Figure S9. Derivative resistance of BTBT-Peptide film between two Au electrodes.

The peptide film thickness was obtained from the AFM images of peptide films scratched by tungsten needles under microscope (Figure S10). The thickness of scratched peptide films was obtained by contact mode imaging using a contact tip with spring constant of 0.2 N/m and resonant frequency of 13 kHz. Images were taken in 80 x 80 um areas at a scan rate of 0.35 Hz, scan angle of 90°, deflection set point of 0.5 V and all images were acquired at a resolution of 512 x 512 points and lines, respectively. Asylum Research MFP-3D model AFM was used for imaging.

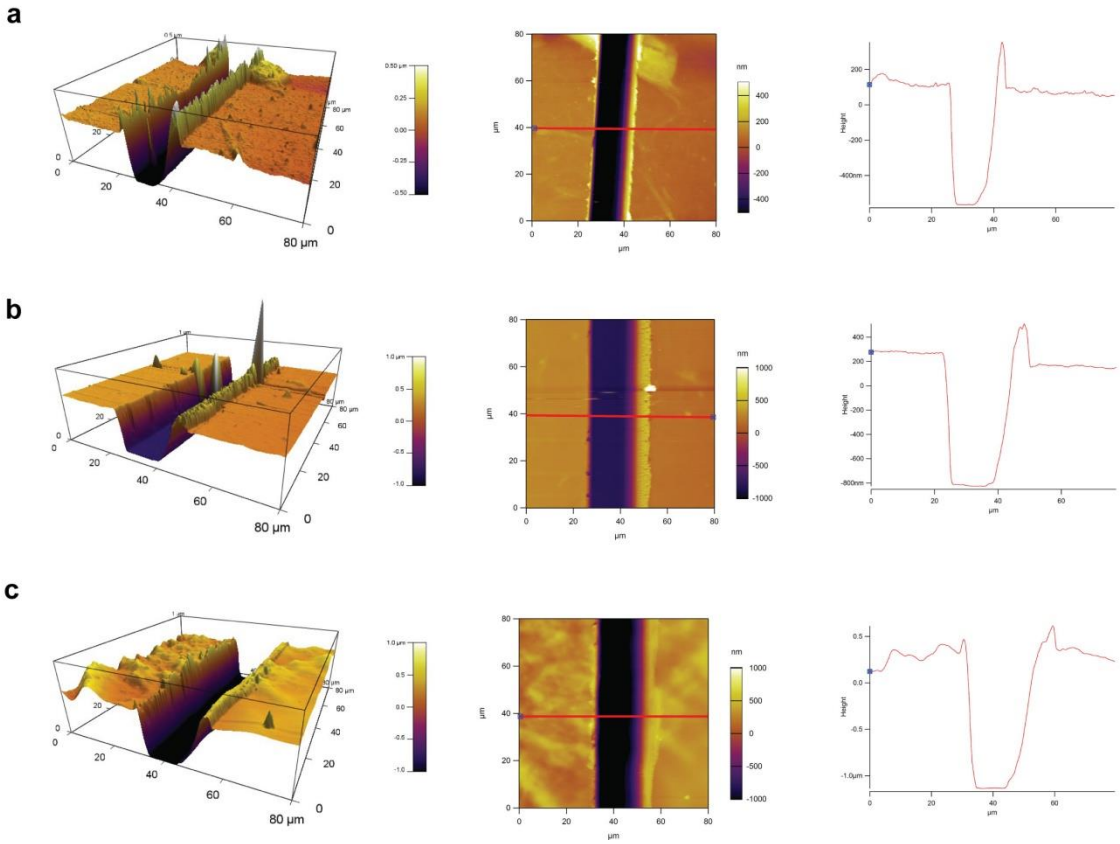

Figure S10. 3D images (left), height retraces (middle) and height profiles (right) of BTBT-peptide film (a), C_8-BTBT-peptide film (b) and BTBT-peptide film with Al contacts (c).

Table S1. Channel dimensions and electrical properties of 7 devices (D) on BTBT-Peptide and C_8-BTBT-Peptide films.

BTBT-Peptide	**D1**	**D2**	**D3**	**D4**	**D5**	**D6**	**D7**
R (MΩ)	11.8	16.6	11.5	9.2	20.3	31.7	8.9
L (μm)	20	20	20	20	20	20	20
W (mm)	4	4	4	4	4	4	4
t (μm)	0.67	0.81	0.88	0.88	1.19	1.15	1.20
ρ (kΩ.m)	1.6	2.7	2.0	1.6	4.8	7.3	2.1
σ (S/cm)	6.3×10^{-6}	3.7×10^{-6}	4.9×10^{-6}	6.2×10^{-6}	2.1×10^{-6}	1.4×10^{-6}	4.7×10^{-6}
C_8-BTBT-Peptide	**D1**	**D2**	**D3**	**D4**	**D5**	**D6**	**D7**
R (MΩ)	630	283	317	399	335	367	670
L (μm)	10	10	10	10	10	10	20
W (mm)	1	1	1	1	1	1	1
t (μm)	0.47	1.59	1.31	1.35	1.30	1.34	1.09
ρ (kΩ.m)	29.7	44.9	41.6	54.0	43.6	49.1	36.4
σ (S/cm)	3.37×10^{-7}	2.23×10^{-7}	2.40×10^{-7}	1.85×10^{-7}	2.30×10^{-7}	2.04×10^{-7}	2.75×10^{-7}

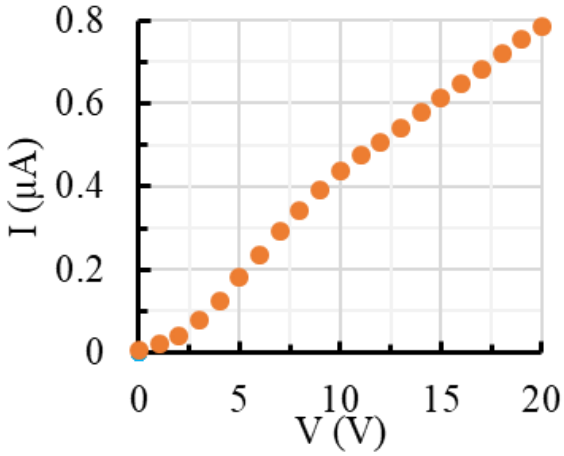

Figure S11. I-V characteristics of BTBT-Peptide film between two Al electrodes.

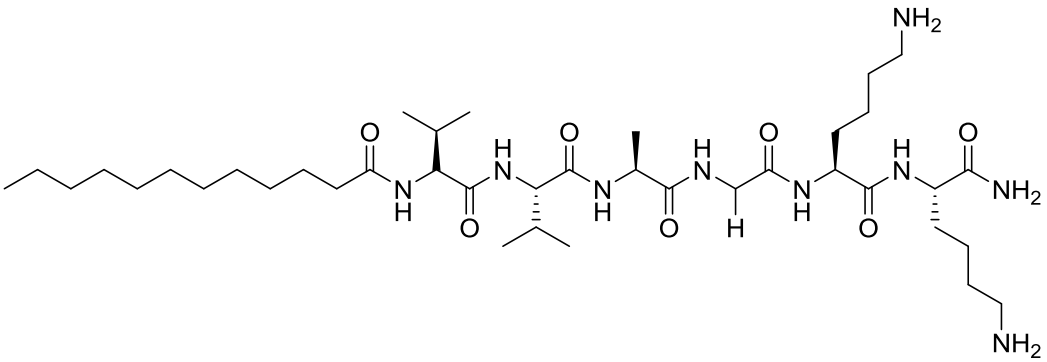

Chemical Formula: $C_{39}H_{75}N_9O_7$
Exact Mass: 781.5789
Molecular Weight: 782.0850

Figure S12. Chemical structure of KK molecule.

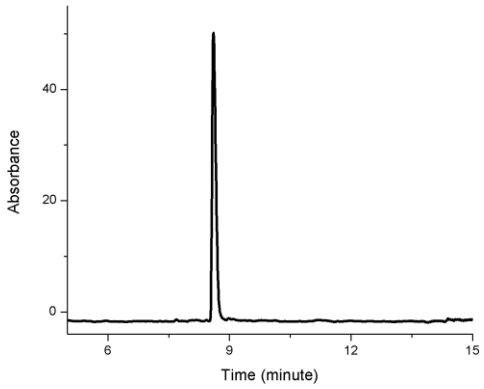

Figure S13. Liquid chromatogram of KK molecule.

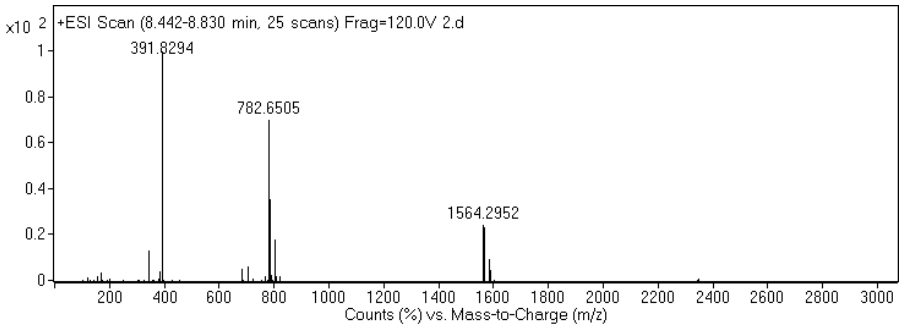

Figure S14. Mass spectrum of KK molecule.

Table S2. Channel dimensions and electrical properties of 6 devices on KK film. The average conductivity value is 1.7×10^{-8} S/cm with $0.6\text{x}10^{-8}$ S/cm standard deviation.

KK	D1	D2	D3	D4	D5	D6
R (GΩ)	2.59	2.04	1.89	2.14	2.1	2
L (μm)	20	20	20	20	20	20
W (mm)	4	4	4	4	4	4
t (μm)	1.6	1.7	0.9	1.3	2.0	1.7
ρ (kΩ.m)	828.8	693.6	340.2	556.4	840.0	680.0
σ (S/cm)	1.2×10^{-8}	1.4×10^{-8}	2.9×10^{-8}	1.8×10^{-8}	1.2×10^{-8}	1.5×10^{-8}